



Article

Warming Climate and Elevated CO₂ Will Enhance Future Winter Wheat Yields in North China Region

Muhammad Rizwan Shoukat ¹, Dongyu Cai ^{2,3}, Muhammad Shafeeqe ^{4,5}, Muhammad Habib-ur-Rahman ^{6,7,*} and Haijun Yan ^{1,8,*}

- ¹ College of Water Resources and Civil Engineering, China Agricultural University, Beijing 100083, China
 - ² College of Resources and Environmental Sciences, China Agricultural University, Beijing 100193, China
 - ³ National Academy of Agriculture Green Development, China Agricultural University, Beijing 100193, China
 - ⁴ Climate Lab, Institute of Geography, University of Bremen, 28359 Bremen, Germany
 - ⁵ International Water Management Institute (IWMI), Lahore 53700, Pakistan
 - ⁶ Institute of Crop Science and Resource Conservation (INRES), University Bonn, 53115 Bonn, Germany
 - ⁷ Department of Agronomy, Muhammad Nawaz Shareef University of Agriculture Multan, Multan 60650, Pakistan
 - ⁸ Engineering Research Center of Agricultural Water-Saving and Water Resources, Ministry of Education, Beijing 100083, China
- * Correspondence: mhabibur@uni-bonn.de (M.H.-u.-R.); yanhj@cau.edu.cn (H.Y.)

Abstract: The projected climate change substantially impacts agricultural productivity and global food security. The cropping system models (CSM) can help estimate the effects of the changing climate on current and future crop production. The current study evaluated the impact of a projected climate change under shared socioeconomic pathways (SSPs) scenarios (SSP2-4.5 and SSP5-8.5) on the grain yield of winter wheat in the North China Plain by adopting the CSM-DSSAT CERES-Wheat model. The model was calibrated and evaluated using observed data of winter wheat experiments from 2015 to 2017 in which nitrogen fertigation was applied to various growth stages of winter wheat. Under the near-term (2021–2040), mid-term (2041–2060), and long-term (2081–2100) SSP2-4.5 and SSP5-8.5 scenarios, the future climate projections were based on five global climate models (GCMs) of the sixth phase of the Coupled Model Intercomparison Project (CMIP6). The GCMs projected an increase in grain yield with increasing temperature and precipitation in the near-term, mid-term, and long-term projections. In the mid-term, 13% more winter wheat grain yield is predicted under 1.3 °C, and a 33 mm increase in temperature and precipitation, respectively, compared with the baseline period (1995–2014). The increasing CO₂ concentration trends projected an increase in average grain yield from 4 to 6%, 4 to 14%, and 2 to 34% in the near-term, mid-term, and long-term projections, respectively, compared to the baseline. The adaptive strategies were also analyzed, including three irrigation levels (200, 260, and 320 mm), three nitrogen fertilizer rates (275, 330, and 385 kg ha^{−1}), and four sowing times (September 13, September 23, October 3, and October 13). An adaptive strategy experiments indicated that sowing winter wheat on October 3 (traditional planting time) and applying 275 kg ha^{−1} nitrogen fertilizer and 260 mm irrigation water could positively affect the grain yield in the North China Plain. These findings are beneficial in decision making to adopt and implement the best management practices to mitigate future climate change impacts on wheat grain yields.

Keywords: climate change; SSPs; CERES-wheat crop model; CMIP6; winter wheat; adaptation technology



Citation: Shoukat, M.R.; Cai, D.; Shafeeqe, M.; Habib-ur-Rahman, M.; Yan, H. Warming Climate and Elevated CO₂ Will Enhance Future Winter Wheat Yields in North China Region. *Atmosphere* **2022**, *13*, 1275. <https://doi.org/10.3390/atmos13081275>

Academic Editor: Tanja Cegnár

Received: 14 July 2022

Accepted: 9 August 2022

Published: 11 August 2022

Publisher's Note: MDPI stays neutral with regard to jurisdictional claims in published maps and institutional affiliations.



Copyright: © 2022 by the authors. Licensee MDPI, Basel, Switzerland. This article is an open access article distributed under the terms and conditions of the Creative Commons Attribution (CC BY) license (<https://creativecommons.org/licenses/by/4.0/>).

1. Introduction

Climate change is accelerating due to rising greenhouse gases concentration in the atmosphere caused by natural, direct, and indirect anthropogenic activities [1–3]. The agriculture industry is the most sensitive to the effects of climate change [4–6], which is a

threat to the food security of a rapidly growing population [7]. According to numerous research studies conducted worldwide, a changing climate is projected to impact agriculture negatively [8,9]. Global warming, changes in precipitation, and higher atmospheric CO₂ concentrations can increase or decrease crop productivity. The total impact of fluctuations in climate on crop yield depends on the combination of these various elements [10]. The most critical climatic factors for crop production are surface temperature and rainfall, which significantly impact agricultural productivity [11–13]. Surface temperatures have risen by 0.5 to 1.3 °C from 1951 to 2010. By the end of the 21st century, global temperatures will increase by 3.7 °C, which will impact food security and crop production positively and negatively around the world [14,15], varying based on the region of interest and adaptation strategies [16,17].

Similar to worldwide trends, agriculture in China is also prone to projected climate change. One of China's most important agricultural production zones is the North China Plain (NCP), accounting for 20.7 percent of the country's total cultivated farmland and more than 70 percent of the country's winter wheat production [18]. Crop yields have been reduced mainly in NCP due to higher temperatures and reduced precipitation [19]. Furthermore, a study of wheat yield data in China from 1979 to 2000 demonstrated that wheat yields declined by around 3 to 10 percent for every 1 °C increase [20]. At the same time, various other studies revealed that a projected increase in precipitation could positively impact grain yield with a temperature rise [21,22]. The projected increase in CO₂ can also be beneficial for increasing wheat grain yield in a warming climate [23,24]. It is critical to ensure the long-term strategies development for better crop production to ensure food security under the projected climate change [25]. It will eventually alter wheat's growth cycle and water requirements, influencing production and quality [26].

Given the higher sensitivity of wheat (*Triticum aestivum* L.) to climate change [7], it is necessary to simulate and project wheat grain yield using a sophisticated crop model. Examining the effects of warming on crop yield will assist farmers in increasing net profits and mitigating risk [27,28]. Various crop simulation models have recently been adopted to evaluate the influence of the ecological risk in agriculture, specifically, the impact of expected climate variability on agriculture yields [29,30]. These models can efficiently simulate the effect of climate variability on crop yield by using a set of genetic coefficients, initial soil conditions, crop management, and meteorological parameters to anticipate crop growth and productivity [31]. These models use climate change scenarios developed from multiple GCMs that account for various climatic considerations. Several studies have used the DSSAT CERES-Wheat model to forecast the effect of changing climate on crop growth and production under different representative concentration pathway (RCP) scenarios [32,33]. It is a CSM that is part of the DSSAT [34,35], which helps to investigate the effects of soil, management of the field (such as fertilizer, irrigation, cultivar, date of planting, and planting density), and climate variability on plant development and yield [32]. The model considers climate, soil, genetic factors, and management options when predicting wheat growth, water balance, nitrogen balance, aboveground biomass, and grain yield [36].

Several studies have been published examining the influence of changing climate on agricultural output under RCP scenarios of GCMs from CMIP5 using the crop modeling approach [33,37–39]. In CMIP5, precipitation intensity was typically underestimated, and spatial resolution was lower than in CMIP6 [40]. Including several new variants and experiments has improved the projected climate in CMIP6 compared to the previous CMIPs [41]. Researchers have found that the new state-of-the-art CMIP6 GCMs can more accurately predict climate extremes by studying biosphere variations due to climate change and understanding how cloud cover affects climate sensitivity compared to CMIP5 models [42]. A key focus of CMIP6 is on coordinating experiments to understand climate variability better, and with CMIP6, potential bias is expected to be minimized to a greater extent than CMIP5 [42]. Recent studies have revealed that CMIP6 GCMs perform better at simulating the climatic indexes in China and other regions [43–46]. However, the climate change

impacts on winter wheat grain yield have not been investigated in depth, which could provide adaptation strategies for sustainable grain production in the future.

The current study hypothesized that the CSM-DSSAT CERES-Wheat model could help examine the future climate change impacts on winter wheat yield in the NCP and decision making for adapting best management strategies based on various crop management practices. According to the projected climate change, the current study can help policymakers in the decision-making process for agricultural sustainability. Therefore, the objectives of the study were to (1) calibrate and evaluate the CSM-DSSAT CERES-Wheat model with an experimental dataset and simulation of phenology, grain yield, total dry-matter, and harvest index; (2) examine the impact of changes in temperature and precipitation on projected winter wheat grain yield under SSP4.5 and SSP8.5 scenarios by using 5 GCMs from CMIP6; and (3) evaluate the effect of projected increasing CO₂ concentration on winter wheat grain yield under various SSP scenarios, developing adaptive strategies to mitigate the adverse impact of a warming climate in the NCP region.

2. Materials and Methods

2.1. Study Area

In the winter wheat growing season from 2015 to 2017, a two-year field study was carried out at the Tongzhou Experimental Station of China Agricultural University located in Beijing, China (39°41′59″ N, 116°41′01″ E; elevation of 21 m). The experimental site is in the NCP (Figure 1) and has warm, temperate, semi-humid, and continental-monsoon weather with an average annual temperature of 11.3 °C. The average yearly precipitation is 620 mm, most of it occurring during summer. The meteorological data were collected from the experimental site using an automatic weather station during the two years of experiments (Figure 2). The soil texture is silt loam; the soil physicochemical properties of the site are provided in Table 1.

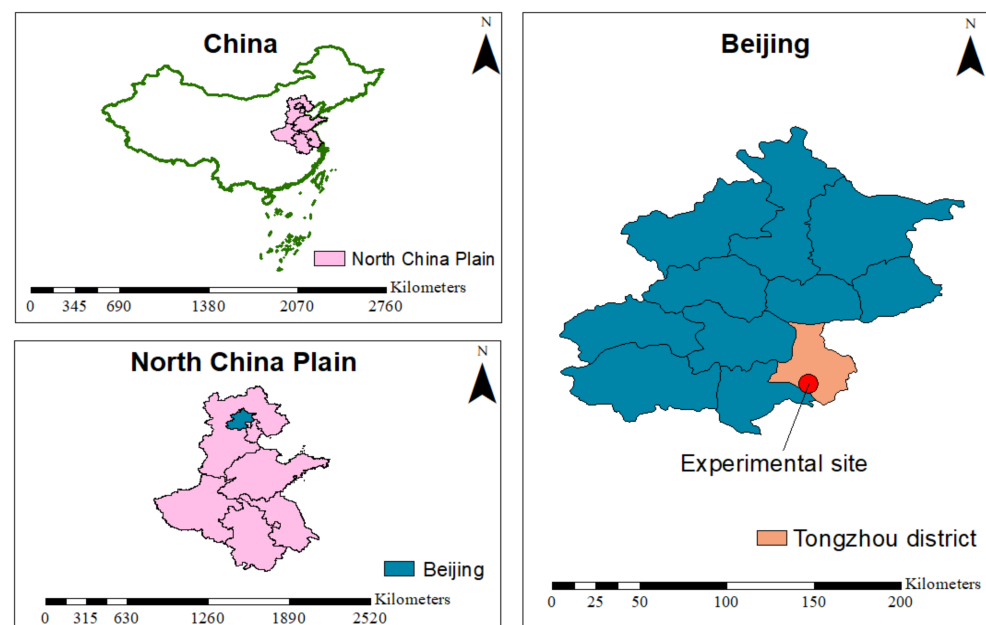


Figure 1. Experimental site location at the Tongzhou experimental station of the China Agricultural University, Beijing, China.

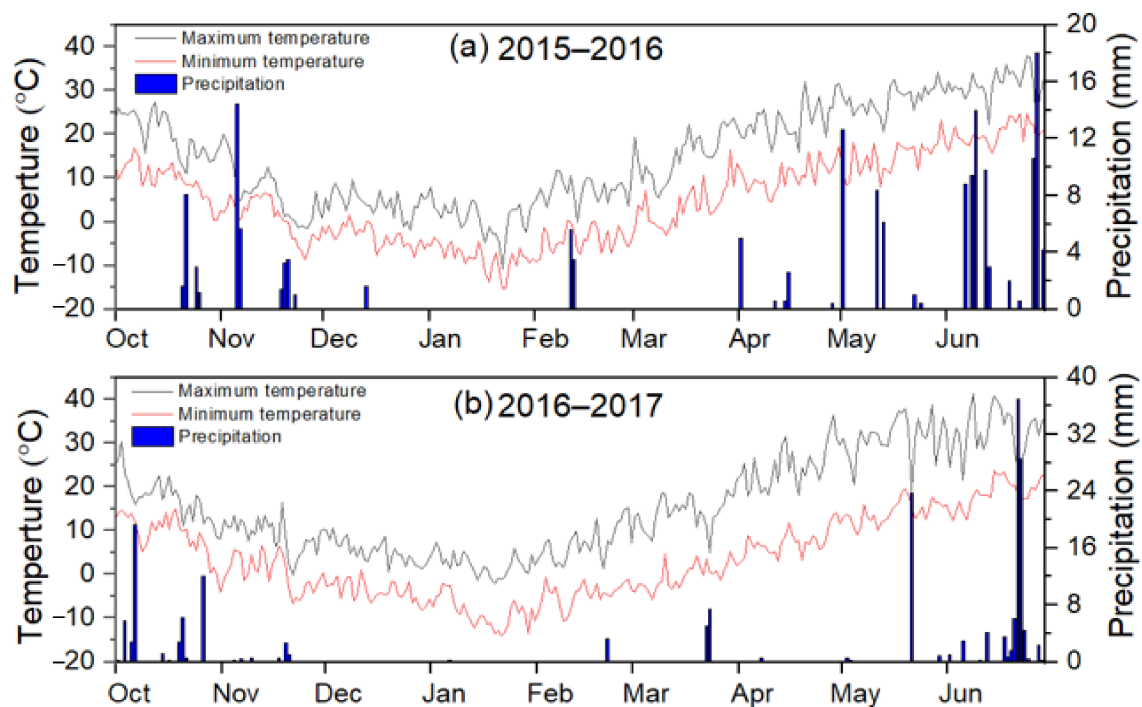


Figure 2. Daily maximum temperature, minimum temperature, and precipitation during (a) 2015–2016 and (b) 2016–2017 winter wheat growing seasons.

Table 1. Soil physicochemical properties of the study area used in CSM CERES-Wheat calibration.

Depth (cm)	Silt (%)	Clay (%)	Bulk Density (g cm ⁻³)	Field Capacity (cm ³ cm ⁻³)	Wilting Point (cm ³ cm ⁻³)	NH ₄ ⁺ -N Content (mg kg ⁻¹)	NO ₃ ⁻ -N Content (mg kg ⁻¹)	Soil Organic Carbon (%)	pH
0–20	52.4	9.2	1.45	0.265	0.099	5.05	17.08	0.99	8.15
20–40	54.8	8.4	1.64	0.267	0.096	3.25	7.94	1.02	8.25
40–60	57.2	7.9	1.64	0.270	0.094	2.80	5.63	0.95	8.29
60–80	63.9	5.5	1.57	0.273	0.084	2.26	6.46	0.88	8.35
80–100	65.7	4.7	1.46	0.273	0.080	2.16	6.35	0.60	8.32

2.2. Experimental Design, Nitrogen Treatments, and Center Pivot Irrigation-Fertigation System

The winter wheat cultivar Nongda 211 was planted on 9 October 2015, and 3 October 2016, with a four-row planter during two-year experiments. The winter wheat was sown at 15 cm row spacing, 4 cm seeding depth, and a 300 kg ha⁻¹ seeding rate. The experiment was conducted under a center-pivot irrigation and fertigation system. The pivot has two-span lengths of 43.3 and 37.5 m for the first and second spans, respectively, and an overhang length of 8.4 m. A P85A impact sprinkler with an 8.7 mm nozzle diameter was installed without a booster pump at the end of the overhang. On the first and second spans, polythene flexible drop pipes were used to install D3000 sprinklers 1.6 m above ground. The upstream of each sprinkler was connected to 15 psi (103 kPa) pressure regulators. The inlet pressure was 240 kPa at the pivot, while the overall system's inlet flow rate was 24.7 m³ h⁻¹.

During the two years of winter wheat experiments, five nitrogen (N) application treatments were applied at different stages, including farmer practice (FP) N application treatment. In the 2015–2016 growing season, the total N fertilizer rate was 315 kg ha⁻¹, from which the basal N fertilizer amount of 108 kg ha⁻¹ was applied, according to the local farmer practice in the study area region. In the 2016–2017 growing season, according to the local average maximum production and crop N requirements, the total N rate was determined as 275 kg ha⁻¹, from which the basal N fertilizer amount of 68 kg ha⁻¹ was

applied. However, in two growing seasons, the amount of topdressing nitrogen fertilizer application was equal and applied at different growth stages (Table 2). A modified tractor-mounted seeding device was used to apply the basal fertilizer to the soil at the sowing time. The source of nitrogen fertilizer was urea (46% N). Based on the Zadoks scale (Z), the stages of crop development were classified [47]. In two years of experiments, topdressing N fertilizer was applied at different growth stages, including the regreening stage (Z25), jointing stage (Z35), anthesis stage (Z60), and filling stage (Z70). In the FP, the broadcasting method was used for one-time N fertilizer (207 kg ha^{-1}) application at the jointing stage. The other four N treatments were applied under the center pivot fertigation system. The center pivot fertigation system comprises a 2000-L tank for storing fertilizer and a piston injection pump capable of flowing 285.5 L per hour. A piston pump injected the urea solution into the irrigation system, then sprinkled it with irrigation water. The winter wheat was irrigated at the overwintering, regreening, jointing, anthesis, and filling stages at a rate of 30 mm, 30 mm, 45 mm, 30 mm, and 30 mm, respectively. However, due to the 29.2 mm of precipitation in November 2015, overwintering irrigation was not carried out in the first growing season. Other field management procedures were followed to promote optimal crop growth throughout the growing season, using the same standards as local fields. The experiments were randomized complete block designs with three replications, and the plots were $6 \text{ m} \times 10 \text{ m}$ in size. The fertigation treatments were applied to the plots in the first, second, and overhanging irrigated areas. The plots of the FP treatment were placed outside the sprinkler area.

Table 2. Topdressing split nitrogen fertilizer application at different growth stages of winter wheat during the 2015–2017 growing seasons.

Years	Treatments	N Frequency	N Rate at Different Growth Stages (kg ha^{-1})			
			Regreening	Jointing	Anthesis	Filling
2015–2016	FP	1	-	207	-	-
	S1	1	-	207	-	-
	S2	2	-	138	-	69
	S3	3	69	103	-	35
	S4	4	69	69	35	34
2016–2017	FP	1	-	207	-	-
	S1	1	-	207	-	-
	S2	2	-	138	-	69
	S3	3	69	103	-	35
	S4	4	69	69	35	34

Note: FP, farmer practice nitrogen application by broadcasting at the jointing stage; S1, one-time nitrogen fertigation at the jointing stage; S2, two split nitrogen fertigations at jointing and filling stages; S3, three split nitrogen fertigations at regreening, jointing, and filling stages; and S4, four split nitrogen fertigations at the regreening, jointing, anthesis and filling stages of winter wheat.

2.3. DSSAT CERES-Wheat Model Description, Calibration, and Evaluation

This study employed the CSM-Crop Environment Resource Synthesis (CERES)-Wheat of the Decision Support System for Agrotechnology Transfer (DSSAT) [34]. A set of variables, such as crop management, climatic conditions, and soil profile parameters, were used in this model to simulate crop development and yield [48]. DSSAT is a powerful tool for analyzing climate change and is widely used [34]. This tool can be used to evaluate crop management strategies at the farm level and crop responses to climate change at the global level. Data needed for DSSAT simulations include crop type, genotype coefficients, sowing, harvest date, plant spacing, fertilizer rates, irrigation levels, tillage operations, soil organic amendments, crop phenology, and grain yield [35,49,50]. The minimum climate data sets were maximum and minimum temperatures, solar radiation, and precipitation. A soil profile's parameters include depth, texture, and chemical and physical characteristics. The study area soil was classified as sandy loam in the model. The information about soil physicochemical properties stored in the soil input file is shown in Table 1. During each

growing season, crop data were collected, including crop phenology, grain yield, total dry matter, and harvest index. For the calibration and evaluation of the DSSAT model, input files, such as weather, crop management, soil, genotype, and A files (average measured data files), were developed. CSM-DSSAT CERES-Wheat model was calibrated and evaluated first so that the grain yield under future climate scenarios could be simulated in the seasonal analysis of the well-calibrated model.

The CERES-Wheat model from DSSAT version 4.8 developed by International Benchmark Sites Network for Agro-technology Transfer Project, Florida, USA was adopted [34]. We collected daily meteorological data, including precipitation, maximum and minimum temperatures, and solar radiation, at our experimental site using an automatic weather station for two years of experiments. The genetic parameters used for the calibration of winter wheat variety “Nongda 211” included the generalized likelihood uncertainty estimation (GLUE) method in DSSAT [51] and the trial and error method [9]. The CERES-Wheat model was calibrated and evaluated with winter wheat data for two growing seasons. Other researchers also used two growing seasons data for CERES-Wheat model calibration and evaluation [52,53]. We calibrated the genetic parameters based on observations of phenological dates (anthesis and maturity dates), total dry matter, grain yield, and harvest index at maturity from minimum stress treatment (S4) in the 2016–2017 growing season [7]. Calibration fits genetic parameters into crop models per local conditions [54]. When new cultivars/hybrids are added, many genetic coefficients must be adjusted according to the local conditions. The calibration process was performed using the field experiments’ five crop parameters (days to anthesis, days to maturity, grain yield, total dry matter, and harvest index). The genetic coefficients adjusted for model calibration are listed in Table 3. After calibration, the CERES-Wheat model was evaluated for wheat phenology, grain yield, dry matter, and harvest index using the other nine treatments from the 2015–2016 and 2016–2017 growing seasons [53]. The model was evaluated with the crop data from other treatments that were not considered in the calibration process. In this study, we applied the well-calibrated DSSAT model to analyze prospective changing climate impacts on winter wheat grain yield under SSPs scenarios for the near-term (2021–2040), mid-term (2041–281), and long term (2081–2100) in the NCP [55].

Table 3. Adjusted winter wheat genetic coefficients for the CSM DSSAT CERES-Wheat model.

Parameter	Definition	Range	Calibrated Value
PIV	The number of days, the optimal vernalizing temperature (d)	5–65	45.45
PID	Responses to the photoperiod	0–95	65.44
P5	Grain-filling stage period (°C d)	300–800	723.80
G1	At anthesis, the number of kernels per unit canopy weight (no. g ^{−1})	15–30	20.50
G2	Size of a standard kernel at optimum conditions (mg)	20–65	29.62
G3	The weight of mature, non-stressed tillers	1–2	1.715
PHINT	Leaf tip appearance interval (°C d)	60–100	71

The model’s accuracy and predictability, such as root mean square error (*RMSE*), percent error (*PE*), normalized root mean square error (*nRMSE*), and Pearson correlation coefficient (*r*), were evaluated [53,56]:

$$RMSE = \sqrt{\frac{1}{n} \sum_{i=1}^n (S_i - O_i)^2} \quad (1)$$

$$PE = \left(\frac{S_i - O_i}{O_i} \right) \times 100 \quad (2)$$

$$nRMSE = \sqrt{\sum_{i=1}^n \frac{(S_i - O_i)^2}{n}} \times \frac{100}{O} \quad (3)$$

$$r = \frac{\sum_{i=1}^n (O_i - \bar{O}) + (S_i - \bar{S})}{\sqrt{\sum_{i=1}^n (O_i - \bar{O})} \sqrt{\sum_{i=1}^n (S_i - \bar{S})}} \quad (4)$$

S_i represents the i -th simulation value, O_i represents the i -th observation value, and n represents the number of samples. O and S with bars are the mean observed and simulated values.

Low *RMSE* is statistically indicative of excellent model performance [57]. The *PE* represents the variation between simulated and experimental data, and the *MAPE* represents the forecasting method's prediction accuracy as a percentage. *PE* and *MAPE* values which are lower, indicate the greater precision and accuracy of the model. The simulation models with lower *PE* or *MAPE* values represent better accuracy and precision [53]. A *nMRSE* value of <10% indicates 'excellent' simulation, $10\% \leq nMRSE < 20\%$ indicates 'good' simulation, $20\% \leq nMRSE < 30\%$ indicates 'fair' simulation and $nMRSE > 30\%$ indicates a 'poor' simulation of the model [58]. Interpretation of the correlation coefficients suggests an r value near 1 or -1 is a perfect correlation between the simulated and observed data values [59].

2.3.1. Seasonal Analysis

The DSSAT seasonal analysis option explores the interaction between genotypes and crop management in different environments, especially under changing climate conditions [35]. In the well-calibrated DSSAT model seasonal analysis, the simulations were run for each unique crop management and weather scenario. In the present study, based on the crop management practices of the optimal treatment (S4, in which topdressing nitrogen fertigation was applied in four split-doses at regreening, jointing, anthesis, and filling stages of winter wheat), seasonal analysis files were generated [60]. In the model, the daily climate data from the historical baseline period (1995–2014) and climate scenarios under SSP2-4.5 and SSP5-8.5 for near-term, mid-term, and long-term were used to prepare weather files of all GCMs. According to the Intergovernmental Panel on Climate Change (IPCC) sixth assessment report, the impact of the expected CO_2 concentration increment on grain yield under SSP1-1.9, SSP1-2.6, SSP2-4.5, SSP3-7.0, and SSP5-8.5 scenarios were analyzed in the seasonal analysis for the near-term, mid-term, and long term [61]. The projected increment in the CO_2 concentration were included in the environmental modification tool in the baseline seasonal analysis file. After analysis, the baseline average grain yield and environmental modification of CO_2 concentration-based average grain yield under various SSPs scenarios were compared. In future scenarios, 165 mm irrigation was applied at the overwintering (30 mm), regreening (30 mm), jointing (45 mm), anthesis (30 mm), and filling (30 mm) stages of winter wheat. The mode of irrigation was a sprinkler irrigation system.

2.3.2. Sixth Phase of Coupled Model Intercomparison Project

Climate change assessments are critical for better understanding the climate system and addressing social hazards and mitigation strategies [44]. For the CMIP6, the Scenario Model Inter-comparison Project (ScenarioMIP) develops a series of predictions for the future climate using simulations based on concentration [62]. In the CMIP6, GCMs were developed with the latest SSPs incorporating greenhouse gas emissions and socioeconomic developments to show future climate [63]. Based on integrated assessment models and alternative predictions of changes in land use and emissions in the future in CMIP6, ScenarioMIP provides multi-model climate projections. Simulations of global climate using the coupled atmosphere-ocean general circulation model (AOGCM) and the Earth system model (ESM) are bundled under the umbrella name GCM as part of CMIP6s [64]. According to the sixth assessment report (AR6) of the IPCC, the updated CMIP6 ensemble holds great potential to evaluate climate change processes and produce updated climate change projections globally, providing a unique exploration of the climate system and its relationship to climate change.

The SSPs are the latest generation of scenarios used in CMIP6 and the IPCC AR6 [61]. These scenarios are part of a new framework for addressing climate change impact, vulnerability, adaptation, and mitigation, which climate change researchers developed. The SSP scenarios in the current study are indicated by SSP1.9, SSP2.6, SSP4.5, SSP7.0, and SSP8.5, respectively. In the SSPs, five themes specify alternative socioeconomic development, including sustainable growth, regional rivalry, inequalities, fossil-fueled improvement, and middle-of-the-road development [65]. The researchers can use the SSPs and associated scenarios to examine the effects of climate change and the corresponding resiliency needs under various socioeconomic growth and climate change scenarios.

2.3.3. Statistical Downscaling and Global Circulation Models

A local perspective on climate change can be challenging to address with GCMs' coarse spatial resolution (approximately 150 km) [66]. Because of this, statistical downscaling is typically used to present fine-scale regional information. The statistical downscaling is based on the relationships between climatic surface variables and large-scale atmospheric variables (usually circulation) [67]. Most agricultural and hydrologic models' climatic outputs and data requirements can be bridged using downscaling, which can be used for local and site-specific climate change implications on crop productivity and food security. The Statistical Downscaling of General Circulation Models (SD-GCM v2.0) software was used in this study. It is a useful tool for downscaling the CMIP6 models' daily, monthly, or yearly climate data under SSP scenarios. Our statistical downscaling approach was based on the delta method, which is widely used with GCM outputs, easy to run, and relatively straightforward [68].

The historical meteorological data for 20 years, including daily precipitation, solar radiation, and maximum–minimum air temperature from 1995 to 2014, were collected from China Meteorological Data Sharing Service System (CMDSSS, <http://cdc.cma.gov.cn>, accessed on 10 October 2021) [69]. The five GCMs were chosen from CMIP6 with SSP4.5 and SSP8.5 scenarios for near-term, mid-term, and long-term periods. These five GCMs were selected based on their climatology; each GCM belongs to a different region [7]. The details of the chosen GCMs of CMIP6 are presented in Table 4. The GCMs climate data under SSP4.5 and SSP8.5 scenarios were obtained from the Earth System Grid Federation (ESGF) website (<https://esgf-node.llnl.gov/search/cmip6/>, accessed on 25 October 2021) [70]. For each GCM in the near-term under SSP4.5, the Taylor diagram [71] was used to represent GCM performance [72] visually. It is a robust graphical plot integrating three statistical measures of Pearson correlation coefficient (r), centered root-mean-square error (CRMSE), and standard deviation (SD) [73].

Table 4. The GCMs of CMIP6 are used for future climate projections under SSP4.5 and SSP8.5 scenarios.

Code	GCM Name	Abbreviation	Institute ID	Country	Climate Zone	Run Used	Atmospheric Model Spatial Resolution
1	ACCESS-CM2	ACC	CSIRO–ARCCSS	Australia	Arid and Tropical	r1i1p1f1	$1.9^{\circ} \times 1.3^{\circ}$
2	CanESM5	CAN	CCCMA	Canada	Continental and Temperate	r1i1p1f1	$2.8^{\circ} \times 2.8^{\circ}$
3	EC-Earth3	ECE	EC–EARTH	Europe	Temperate	r1i1p1f1	$0.7^{\circ} \times 0.7^{\circ}$
4	GFDL-ESM4	GFD	GDFL	USA	Continental	r1i1p1f1	$1.0^{\circ} \times 1.2^{\circ}$
5	MIROC6	MIR	MIROC	Japan	Sub-tropical	r1i1p1f1	$1.4^{\circ} \times 1.4^{\circ}$

2.3.4. Projections of Climate Change Impact and Adaptive Management Scenarios for Winter Wheat Production in a Warming Climate

Future climate projections provide information on the climate system and data products used in climate impact assessments [74]. In the near-term, mid-term, and long-term climate change projections, the winter wheat grain yield in NCP was analyzed using a

CSM-DSSAT CERES-Wheat seasonal analysis tool [7,60]. The current study focused on the projected daily maximum and minimum temperature and precipitation under SSP4.5 and SSP8.5 scenarios, while it was assumed that all other atmospheric parameters would remain unchanged. A similar approach was used by other researchers as well [4,9,52]. The weather files were created in the CERES-Wheat model using daily baseline climate data (1995–2014) [75] and daily future climate data of GCMs under SSP4.5 and SSP8.5 scenarios for near-term, mid-term, and long term. According to IPCC-AR6, expected CO₂ concentration increases under SSP1.9, SSP2.6, SSP4.5, and SSP8.5 scenarios were also evaluated in the environmental modification tool in the CERES-Wheat model. The projected CO₂ concentration increment for the near-term, mid-term, and long-term period under SSP1.9, SSP2.6, SSP4.5, and SSP8.5 scenarios [61] were used in the environmental modification of the baseline management file in the seasonal analysis tool (Supplementary Table S1). The historical climate data (1995–2014) were used as the baseline climate data, and the default concentration of CO₂ 380 ppm in the DSSAT model was considered the baseline level. Various other studies also used a similar approach to investigate the impact of CO₂ on grain yield under RCP scenarios [7,9].

The following equation was used to determine the influence of changing climate on winter wheat grain yields:

$$\Delta Y = \left(\frac{Si - Oi}{Oi} \right) \times 100 \quad (5)$$

where ΔY is the change in grain yield, Si is the average future expected, and Oi is the average observed grain yield in the baseline period.

The adaptive strategies to mitigate the adverse impact of the warming climate on winter wheat grain yield were examined in the seasonal analysis of the well-calibrated CSM CERES-Wheat model [4,9,52]. The 20-year climate data (maximum temperature, minimum temperature, and precipitation) in the near-term of GCM were used to develop adaptation strategies to reduce the negative impact of a warming climate on winter wheat grain yield. The GCM that predicted the decrease in grain yield with the rise in temperature and reduced precipitation in the near-term than the historical baseline period was selected. The model evaluated the sowing times, nitrogen application rates, and irrigation amounts to establish the optimal management practices for future winter wheat production under a warming climate. The irrigation water (W) amounts of 200 mm (FP) [76], 260 mm (30% more than FP), 320 mm (60% more than FP), and N fertilizer rates of 275 kg ha^{−1} (FP) [77], 330 kg ha^{−1} (20% more than FP), and 385 kg ha^{−1} (40% more than FP) were analyzed under four sowing times (13 September, 23 September, 3 October, and 13 October). The sowing dates were designed at 10-day intervals according to the recommended and traditional sowing in early October in NCP (October 3 was considered a recommended sowing date in adaptive strategies management) [78]. The grain yield was compared in nine combinations of irrigation water and N fertilizer management scenarios (3 irrigation water and 3 N fertilizer levels) under four sowing dates to develop the optimal management strategy for enhancing winter wheat grain yield in a warming climate.

3. Results

3.1. DSSAT CERES-Wheat Model Calibration and Evaluation

The model was calibrated with minimal stress-based optimal treatment (S4), in which the maximum grain yield was also observed in the 2016–2017 wheat growing season. The genetic coefficients of the model were recalculated to match the simulated and measured data. In the wheat cultivar file of the model, the coefficients were determined through several iterations such that observed and simulated values of phenology and yield were close to each other. The estimated genetic coefficients for PIV, PID, P5, G1, G2, G3, and PHINT were 45.45, 65.44, 723.80, 20.50, 29.62, 1.715, and 71, respectively (Table 3). The model's calibration results showed that it performed well in simulating phenology, grain yield, total dry matter, and harvest index. During the calibration process, the simulated maturity date was the same as the observed date with no *PE*. The *PE* between simulated

and observed anthesis date, grain yield, total dry matter, and HI were 0.47%, 1.15%, 0.33%, and 0.73%, respectively (Supplementary Table S2). The lower *PE* showed that the CERES-Wheat model was calibrated successfully with a reliable result according to the study area environment.

Further evaluation of the calibrated CSM DSSAT-CERES-Wheat model was conducted with field data from the other treatments of both years of the experiment, which was not considered in the calibration process, as described in the following section.

3.1.1. Model Performance for Nitrogen Application Effects on Winter Wheat Phenology

The simulations were consistent with observed days to anthesis, with an average *PE* of 1.92% and 0.47% in the 2015–2016 and 2016–2017 growing seasons, respectively (Supplementary Table S2). At the same time, the average *PE* days to maturity were 0.8% and 0 in the 2015–2016 and 2016–2017 growing seasons, respectively. The *RMSE* of days to anthesis were 4 and 1 days, and days to maturity were 2 and 0 days in the 2015–2016 and 2016–2017 growing seasons, respectively. While *nRMSE*, days to anthesis were 2% and 0.5%, and days to maturity were 0.8% and 0 in the 2015–2016 and 2016–2017 growing seasons, respectively (Table 5).

Table 5. DSSAT CERES-Wheat model performance simulates crop phenology, grain yield, total dry matter, and harvest index during 2015–2016 and 2016–2017.

Year	Parameter	Anthesis Date (DAP)	Maturity Date (DAP)	Grain Yield (kg ha ⁻¹)	Total Dry Matter (kg ha ⁻¹)	Harvest Index
2015–2016 (<i>n</i> = 5)	<i>RMSE</i>	4.00	2.00	239.83	733.49	0.02
	<i>nRMSE</i> (%)	2.00	0.80	3.00	3.70	5.30
	<i>r</i>	-	-	0.94	0.59	0.88
2016–2017 (<i>n</i> = 4)	<i>RMSE</i>	1.00	0.00	137.64	745.75	0.02
	<i>nRMSE</i> (%)	0.50	0.00	1.60	3.50	4.60
	<i>r</i>	-	-	0.97	0.94	0.47

Note: *n*, number of treatments, DAP, days after planting; *RMSE*, root mean square error; *nRMSE*, normalized root mean square error; *r*, Pearson correlation coefficient.

3.1.2. Model Performance for Nitrogen Application Effects on Grain Yield

During both growing seasons, 2015–2016 and 2016–2017, simulated grain yields were very close to observed yields. The average *PE* recorded for grain yield in the 2015–2016 and 2016–2017 growing seasons were 1.33% and 0.56%, respectively (Table S2). During 2015–2016, *PE* ranged from 3.16 to 4.63 %, and in 2016–2017 it was from 1.15 to 2.97%. The *RMSE* values for grain yield were 238.83 and 137.64 kg ha⁻¹ in 2015–2016 and 2016–2017. Model performance was better in the lower *RMSE*. The *nRSME* and *r* values were 3% and 0.94 in 2015–2016, and 1.60% and 0.97 in the 2016–2017 winter wheat season (Table 5). The lower *nRMSE* indicated that the observed and model-simulated values were close to each other.

3.1.3. Model Performance for Nitrogen Application Effects on Total Dry Matter

The simulated and observed values for total dry matter with different split nitrogen applications were in good agreement. In the 2015–2016 and 2016–2017 growing seasons, the average *PE* recorded for the total dry matter was 2.59% and 2.57%, respectively (Table S2). Minimum *PE* was recorded in 2015–2016, ranging from 1.75 to 5.99% and 1.03 to 7.59% in the 2016–2017 growing season. In 2015–2016 and 2016–2017, the *RMSE* values for total dry matter were 733.49 and 745.75 kg ha⁻¹, respectively. For winter wheat season 2015–2016, the *nRSME* and *r* values were 3.70%, and 0.59, while 3.50% and 0.94 were in 2016–2017 (Table 5). Observed and model-simulated values were as close as possible, due to the lower *RMSE* and *nRMSE*.

3.1.4. Model Performance for Nitrogen Application Effects on Harvest Index

Based on different split nitrogen applications, the simulated and observed values of the harvest index were in good agreement. The average *PE* for the harvest index in the growing seasons of 2015–2016 and 2016–2017 were 3.38% and 3.17%, respectively (Table S2). The *RSME* values were 0.021 and 0.018 in the 2015–2016 and 2016–2017 growing seasons. In the winter wheat growing season of 2015–2016, the *nRSME* and *r* were 5.30% and 0.88, respectively, while they were 4.60% and 0.47, respectively, in 2016–2017 (Table 5).

3.2. Climate Change Impact on Grain Yield in the Near-Term, Mid-Term, and Long-Term under Global Climate Models

The current study predicted future winter wheat grain yields in response to climate change in the near-term, mid-term, and long-term using five GCMs and two SSPs datasets (SSP4.5 and SSP8.5) of CMIP6 (Figures 3–5). Mostly, the GCMs showed an increase in average grain yield under climate change. The changes in average maximum temperature (*Tmax*), minimum temperature (*Tmin*), and precipitation (*Pr*) in the near-term, mid-term, and long-term under SSP4.5 and SSP8.5 scenarios are shown in Table 6, compared with the baseline period. The average maximum temperature of 13.7 °C, minimum temperatures of 3.4 °C, and average seasonal precipitation of 147 mm were observed during the baseline period. Overall, from all the GCMs, the average maximum grain yield of 9211 kg ha^{−1} was noticed in the ACCESS-CM2 model in the near-term under the SSP8.5 scenario with a projected 0.9 °C rise in the average minimum, 1.0 °C in the maximum temperature, and 48 mm increase in precipitation, compared with the baseline period (7190 kg ha^{−1}). Meanwhile, in the mid-term (2041–2060), GFDL-ESM4 forecasted the highest average grain yield of 9084 kg ha^{−1} under the SSP4.5 scenario with 0.7 °C rises in each average maximum and minimum temperature, and 66 mm increase in the average seasonal precipitation, compared with the baseline period (7190 kg ha^{−1}). In the long term, GFDL-ESM4 GCM projected the highest average grain yield of 8783 kg ha^{−1} under the SSP4.5 scenario with increases of 1.3 °C in minimum temperature, 1.1 °C in maximum temperature and 59 mm in average seasonal precipitation, compared with the baseline period (7190 kg ha^{−1}).

Table 6. Changes in the winter wheat seasonal mean of climate projections of five GCMs in the near-term, mid-term, and long-term.

Near-Term: 2021–2040						
GCMs	SSP4.5			SSP8.5		
	<i>Tmax</i> (°C)	<i>Tmin</i> (°C)	<i>Pr</i> (mm)	<i>Tmax</i> (°C)	<i>Tmin</i> (°C)	<i>Pr</i> (mm)
ACCESS-CM2	0.6	0.8	43.1	1	0.9	48
CanESM5	0.6	0.8	−4.5	0.4	0.8	29.5
EC-Earth3	1.2	0.8	−51.5	1.2	0.9	−39.5
INM-CM5-0	1.1	0.1	37.5	1.3	0.1	41.5
MIROC6	0.4	0.3	52.5	0.8	0.5	55.5
Mid-term: 2041–2060						
ACCESS-CM2	1.7	1.7	39.5	1.6	1.6	20.5
CanESM5	1.1	1.5	64.5	1.6	2	22.5
EC-Earth3	1.4	1.3	−12.5	1.8	1.7	20.5
INM-CM5-0	1.5	0.2	43.5	1.6	0.6	49.5
MIROC6	0.6	0.7	38.5	1	1	36.5
Long-term: 2081–2100						
ACCESS-CM2	2.1	2.1	8.5	3.2	3.7	46.5
CanESM5	1.5	2	64.5	3.9	4.5	10.5
EC-Earth3	2	1.9	−16.5	3.2	3.7	3.5
INM-CM5-0	1.4	0.4	42.5	2.5	1.5	10.5
MIROC6	1.1	1.1	27.5	2	2.5	35.5

Note: *Tmax*, maximum temperatures; *Tmin*, minimum temperature; and *Pr*, precipitation (−ve sign shows the reduction in precipitation).

The grain yield across all GCMs based on maximum and minimum temperature and precipitation changes under SSP4.5 and SSP8.5 scenarios differed in the near-term, mid-term, and long-term. In the near-term, under the SSP4.5 scenario, GCMs forecasted a 9% more average grain yield with a 0.7 °C increase in average minimum and 0.8 °C in maximum temperature and a 17 mm rise in average seasonal precipitation compared to the baseline period. In the mid-term, with a 1.3 °C rise in each average maximum and minimum temperature and a 33 mm increase in precipitation, most GCMs predicted a 13% more average grain yield than the baseline period. While in the long-term, a 3% increase in average grain yield was observed with an increase of 2.5 °C in average minimum temperature and 2.2 °C in average maximum temperature, and a 29 mm increase in precipitation compared to the baseline period. These findings proposed that the increased precipitation can counteract the warming climate impact and increase the winter wheat grain yield. According to most of the GCMs predictions, the winter wheat yield is likely to increase significantly in the near-term and mid-term under the SSP4.5 and SSP8.5 scenarios due to the increase in precipitation with increasing temperature than the baseline period.

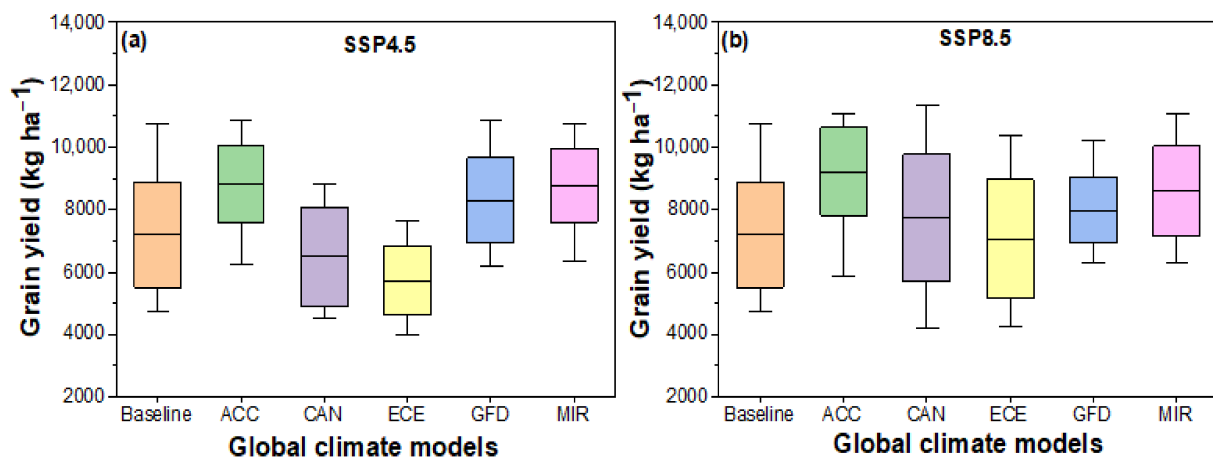


Figure 3. Projected winter wheat grain yield for near-term under SSP4.5 (a) and SSP8.5 (b) scenarios of five GCMs. ACC represents ACCESS-CM2, CAN represents CanESM5, ECE represents EC-Earth3, GFD represents GFDL-ESM4, and MIR represents MIROC6 GCM. The baseline period is from 1995 to 2014.

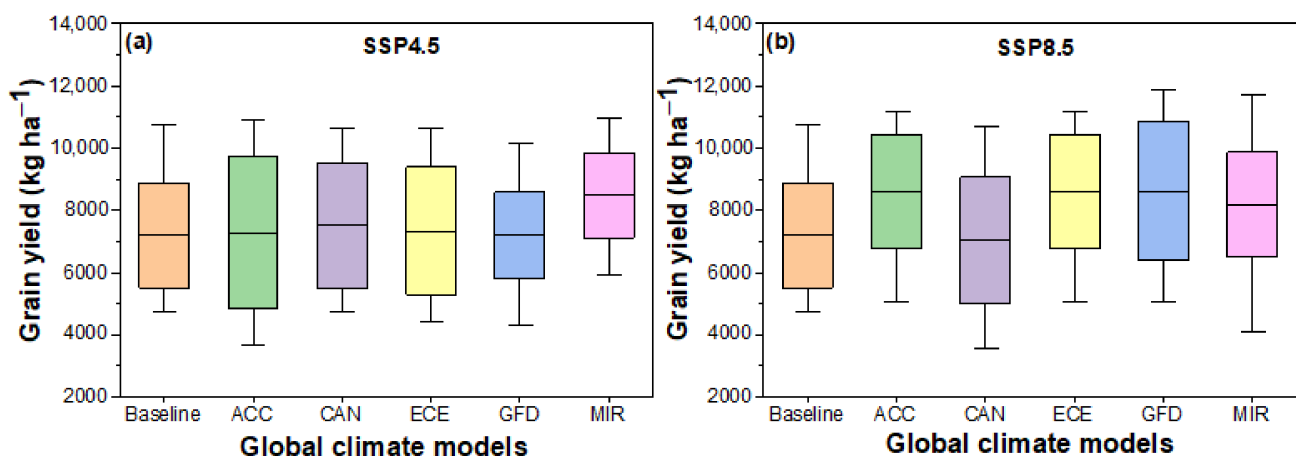


Figure 4. Projected winter wheat grain yield for mid-term under SSP4.5 (a) and SSP8.5 (b) scenarios of five GCMs. ACC represents ACCESS-CM2, CAN represents CanESM5, ECE represents EC-Earth3, GFD represents GFDL-ESM4, and MIR represents MIROC6 GCM. The baseline period is from 1995 to 2014.

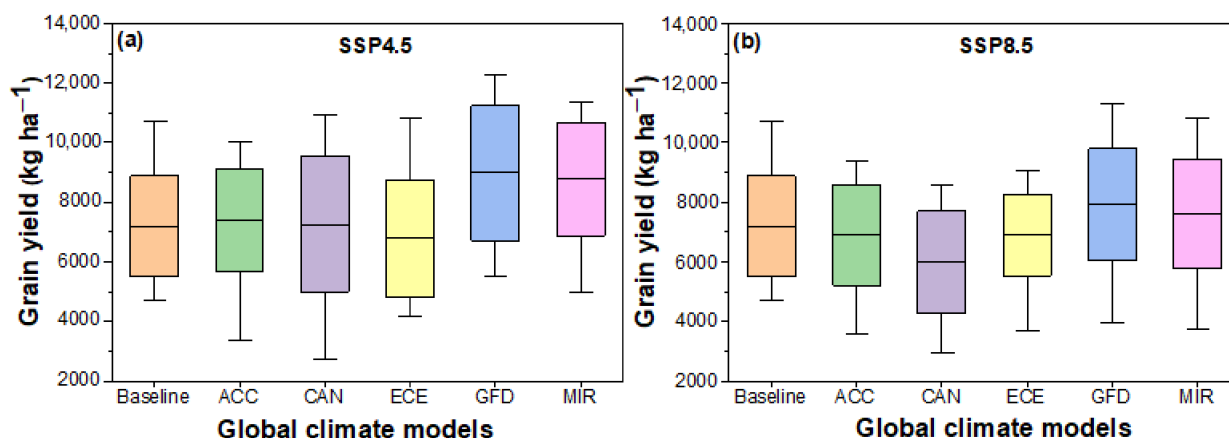


Figure 5. Projected winter wheat grain yield for long-term under SSP4.5 (a) and SSP8.5 (b) scenarios of five GCMs. ACC represents ACCESS-CM2, CAN represents CanESM5, ECE represents EC-Earth3, GFD represents GFDL-ESM4, and MIR represents MIROC6 GCM. The baseline period is from 1995 to 2014.

3.3. Effect of CO₂ Concentrations Scenarios on Future Winter Wheat Grain Yield

A model's response to CO₂ concentration in the near-term, mid-term, long-term, and baseline period (1995–2014) is presented in Figures 6–8. According to the sixth assessment report of IPCC, the increase in CO₂ concentrations in the near-term, mid-term, and long-term is shown in Table S1. The increase in grain yield was observed as the CO₂ concentration increased in the near-term, mid-term, and long-term scenarios compared to the baseline CO₂ level (380 ppm) in the baseline climate data. The average maximum grain yield of 7590 kg ha^{−1} and minimum grain yield of 7446 kg ha^{−1} was under the SSP8.5 CO₂ concentration scenario (456 ppm) and the SSP4.5 scenario (429 ppm), respectively, in the near-term. In the mid-term (2041–2060), the average maximum and minimum grain yield was 8161 kg ha^{−1} and 7480 kg ha^{−1} under the SSP8.5 and SSP1.9 scenarios, respectively, compared to the baseline level yield (7190 kg ha^{−1}). During the long term (2081–2100), the minimum and maximum average grain yields were 7325 kg ha^{−1} and 9601 kg ha^{−1} under the SSP1.9 and SSP8.5 scenarios, respectively, compared to the baseline average grain yield (7190 kg ha^{−1}).

It should be noted that there was no substantial difference in grain yield among all CO₂ concentration scenarios (SSP1.9, SSP2.6, SSP4.5, SSP7.0, and SSP8.5) in the near-term due to the lower projected CO₂ concentration than mid-term and long-term. However, compared to the baseline average grain yield, a 4 to 6% increase in average grain yield was observed in the near-term. In the mid-term, 4 to 14% more average grain yield was noticed under the increasing CO₂ concentration scenarios. However, the CO₂ concentration scenarios in the long-term demonstrated a significant increase in the average grain yield from 2 to 34% due to the higher rise in CO₂ concentration than the baseline period. The increasing concentration of CO₂ in the future can positively affect the winter wheat grain yield in a warming climate.

3.4. Optimal Management Scenario for Winter Wheat under a Warming Climate and Taylor Diagram

The irrigation water and N fertilizer management scenarios positively affected the grain yield under various sowing dates in a warming climate of the near-term (Figures 9–12). The EC-Earth3 daily climate data, including maximum temperature, minimum temperature, and precipitation, were used to develop adaptive strategies to mitigate the warming climate impact on winter wheat grain yield. The average maximum grain yield of 9676 kg ha^{−1} was observed on 260 mm irrigation water and 275 kg ha^{−1} N fertilizer application (W260N275) with sowing winter wheat at the recommended sowing time (the first week of October and 3 October was used in this study). It was 74% higher than the EC-Earth3 average

grain yield (5885 kg ha^{-1} , without any management strategy to mitigate the warming climate impact on grain yield) in the near-term. The average minimum grain yield was 5841 kg ha^{-1} , noticed with the 200 mm irrigation water and 385 kg ha^{-1} N fertilizer management scenario (W200N385) under sowing on 23 September. It was also noticed that a higher level of irrigation water and N fertilizer rate did not enhance the grain yield under all sowing dates. In this study, 320 mm irrigation water and 385 kg ha^{-1} N fertilizer application (W320N385) showed a 6696 kg ha^{-1} grain yield, which was 45% lower, compared with the grain yield in 260 mm irrigation water and 275 kg ha^{-1} N fertilizer application (W260N275) under sowing on 3 October. Overall, this study found that sowing winter wheat on 3 October and applying 260 mm irrigation water, and 275 kg ha^{-1} N fertilizer can be optimal management strategies for mitigating the adverse impact of the warming climate on winter wheat grain yield in the near-term.

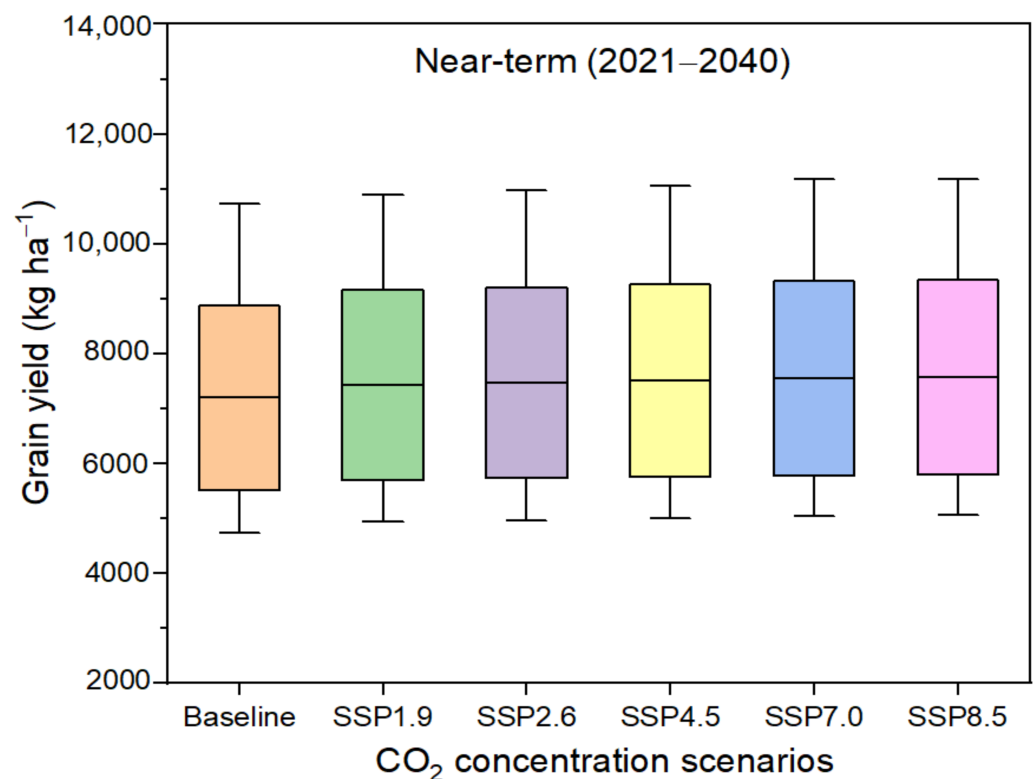


Figure 6. Effect of CO₂ concentration increasing scenarios for near-term on projected winter wheat grain yield under various SSPs scenarios, compared to the baseline period. In the SSP1.9, SSP2.6, SSP4.5, SSP7.0, and SSP8.5 scenarios, the CO₂ concentrations are 429, 437, 444, 453, and 456 ppm, respectively.

The GCM performance was also analyzed in the near-term using the Taylor diagram. The Pearson correlation was examined between GCMs and historical baseline climate data (Supplementary Figure S1). On the x-axis, Ref = 1 represents the reference data (historical climate data from 1995 to 2014). The maximum Pearson correlation of 0.89 was observed for the maximum and minimum temperatures in ACCESS-CM2 under the SSP4.5 scenario. However, CanESM5 and ACCESS-CM2 demonstrated a higher Pearson correlation of 0.11 for precipitation under the SSP4.5 scenario. This study found that the ACCESS-CM2 can be the best GCM for the maximum and minimum temperatures and CanESM5 for the precipitation simulation in the near-term.

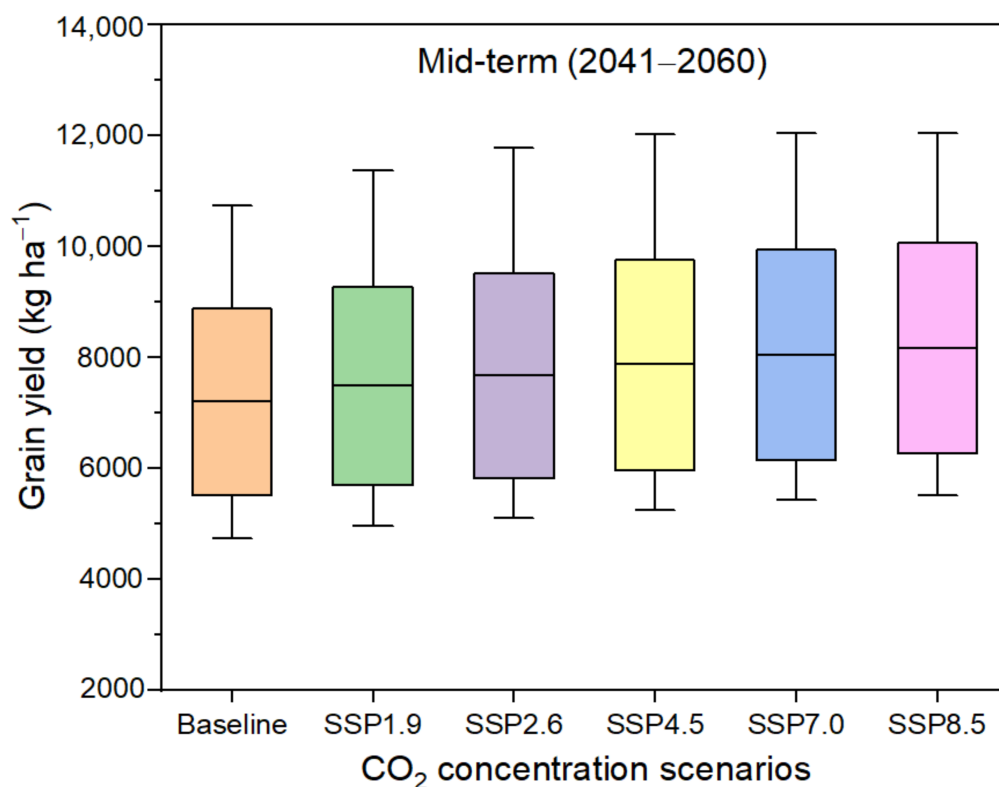


Figure 7. Effect of CO₂ concentration increasing scenarios for mid-term on projected winter wheat grain yield under various SSPs scenarios compared to the baseline period. In the SSP1.9, SSP2.6, SSP4.5, SSP7.0, and SSP8.5 scenarios, the CO₂ concentrations are 436, 467, 506, 542, and 569 ppm, respectively.

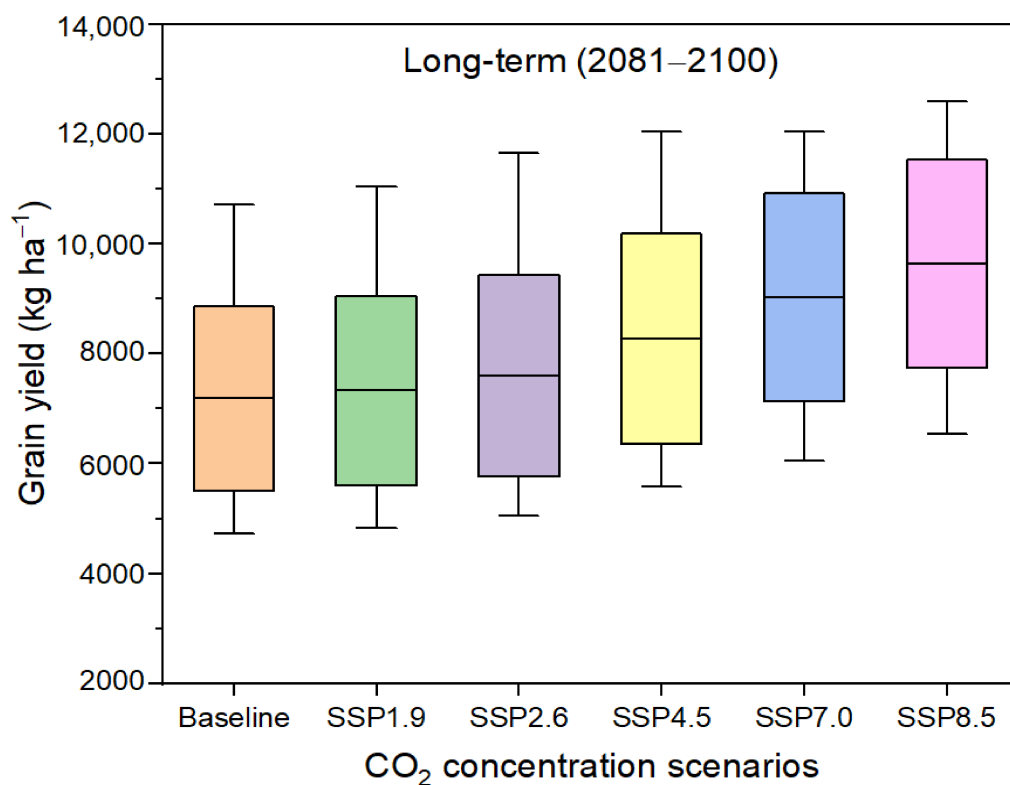


Figure 8. Effect of CO₂ concentration increasing scenarios for long-term on projected winter wheat grain yield under various SSPs scenarios compared to baseline period. In the SSP1.9, SSP2.6, SSP4.5, SSP7.0, and SSP8.5 scenarios, the CO₂ concentrations are 405, 457, 595, 790, and 999 ppm, respectively.

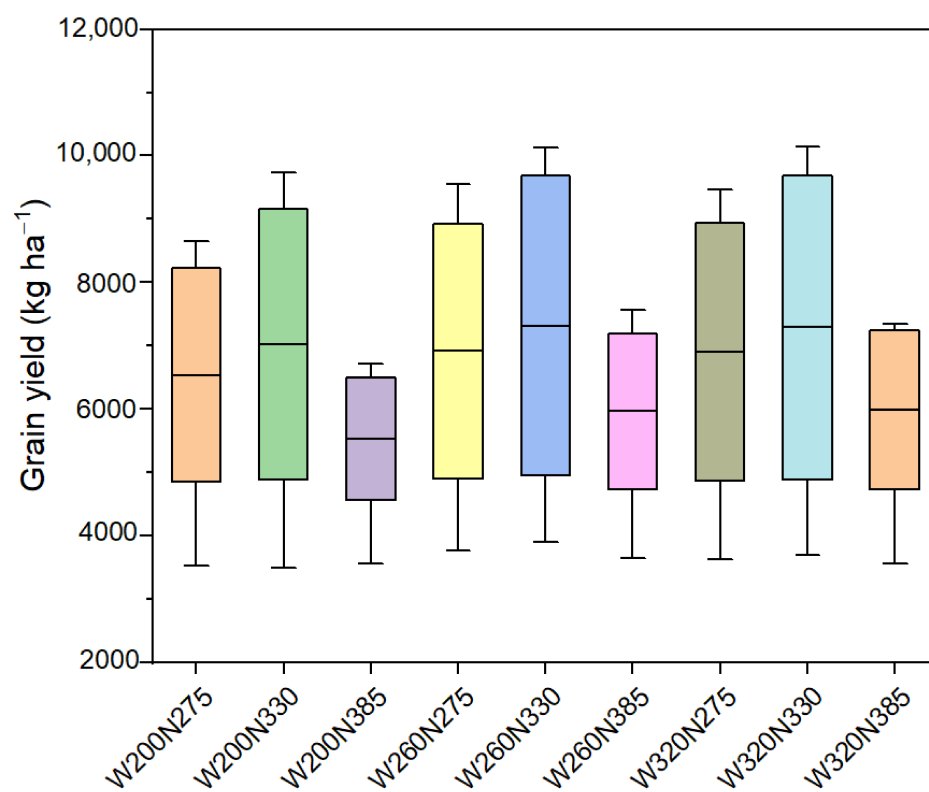


Figure 9. Effects of various irrigation management scenarios on winter wheat grain yield under sowing on 13 September in a warming climate. W with values represents the irrigation water amount in mm, and N values are nitrogen fertilizer rates in kg ha⁻¹.

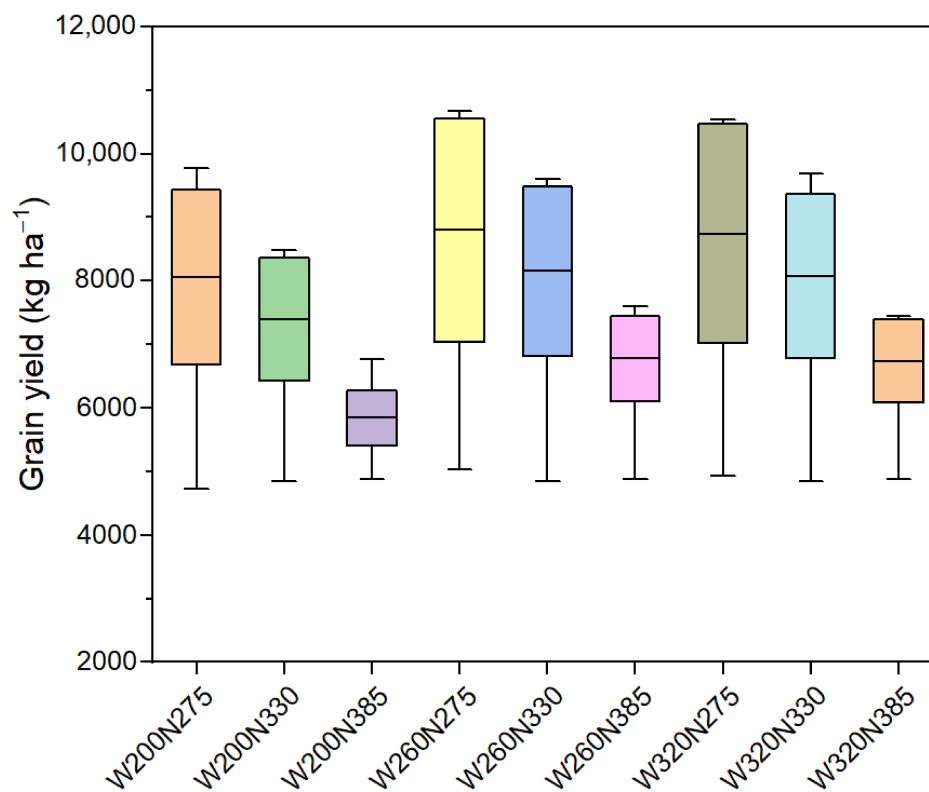


Figure 10. Effects of various irrigation management scenarios on winter wheat grain yield under sowing on 23 September in a warming climate. W with values represents the irrigation water amount in mm, and N values are nitrogen fertilizer rates in kg ha⁻¹.

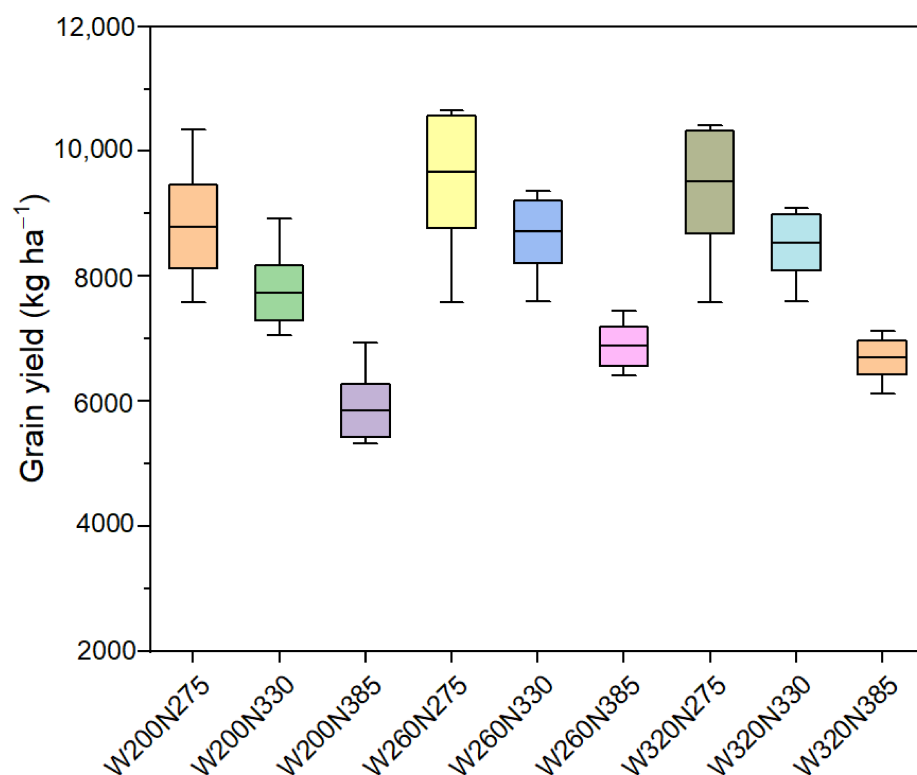


Figure 11. Effects of various irrigation management scenarios on winter wheat grain yield under sowing on 3 October in a warming climate. W with values represents the irrigation water amount in mm, and N values are nitrogen fertilizer rates in kg ha⁻¹.

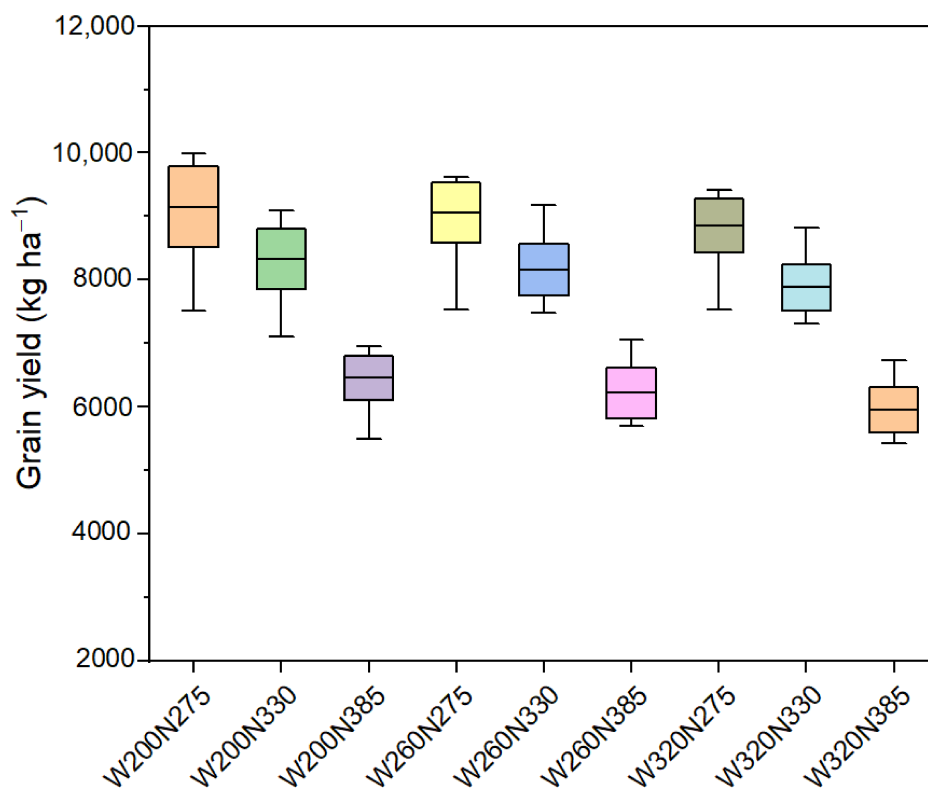


Figure 12. Effects of various irrigation management scenarios on winter wheat grain yield under sowing on 13 October in a warming climate. W with values represents the irrigation water amount in mm, and N values are nitrogen fertilizer rates in kg ha⁻¹.

4. Discussion

In the current study, we calibrated and evaluated the DSSAT-CERES-Wheat model with field crop data for two growing seasons. The observed data for two growing seasons are enough for CERES-Wheat model calibration and evaluation. Several researchers used two seasons in their studies to calibrate and validate the crop model [52,53]. The model demonstrates good performance in simulating days to anthesis, days to maturity, grain yield, total dry matter, and harvest index, as shown in Table 5. Our findings are consistent, as reported in previous studies [7,53,79,80]. Simulations of anthesis and maturity dates were close to the observed dates, with *PE* and *nRMSE* of less than 5%, and the *RMSE* was less than five days in all treatments in both seasons of experiments. Timsina and Humphreys [81] observed the *nRMSE* of 4 to 5% anthesis and maturity time in the CERES-Wheat model. Feng et al. [82] noticed *RMSE* of 1.83 and 3.56 days for winter wheat anthesis and maturity time. The average *RMSE* values were less than 300 kg ha⁻¹, 800 kg ha⁻¹, and 0.03, and average *r* values were 0.95, 0.77, and 0.68 for grain yield, total dry matter, and harvest index, respectively, in both growing seasons. Meanwhile, the *nRMSE* values were less than 10% in all treatments in two years of the experiment for grain yield, total dry matter, and harvest index. Our findings are consistent with the Malik and Dechmi [83] study, which reported a *nRMSE* of less than 10% for the simulated yield in the CSM CERES-Wheat model. The calibrated model was then used to analyze the climate change impact assessment on wheat yields.

Five GCMs were selected for forcing the calibrated crop model because a single GCM cannot be relied upon in climate change impact studies [52,84]. Multiple models may effectively assess the climate change's impact on crop yield [9,85]. In the study, most GCMs predicted a rise in projected temperature and increased precipitation in the near-term, mid-term, and long-term with an increase in grain yield compared to the baseline period (1995–2014). Lopes [21] also observed that increasing precipitation and temperature favor wheat growth and photosynthesis, resulting in increased grain yield. In the near-term, ACCESS-CM2 GCM showed a 28% more average grain yield under the SSP8.5 scenario with 1.0 °C rises in each average maximum and 0.9 °C minimum temperature and a 29% increase in seasonal precipitation compared to the baseline average grain yield (1995–2014). The rainfall might be a primary factor that counteracts temperature-induced adverse effects on crop yield, which is in agreement with Kukal and Irmak's [86] observations. It shows that the rise in temperature and increased precipitation can be beneficial for increasing the winter wheat grain yield [87]. This study also found that the increase in temperature and reduction in precipitation can adversely impact the winter wheat grain yield, consistent with the findings of Zhao et al. [88]. The increasing temperature and decreasing precipitation will increase daily crop water consumption; crop growth and development are expedited by higher temperatures, which can adversely impact crop production [89]. This study finding suggests that the projected increasing precipitation trend with rising temperature in the near-term, mid-term, and long-term under SSP4.5 and SSP8.5 scenarios can compensate for the warming climate impact on winter wheat grain yield.

The winter wheat average grain yield increased with increasing CO₂ under all SSPs scenarios of CMIP6 in the near-term, mid-term, and long term. Various researchers observed similar findings [4,9,90]. Kimball et al. [91] reported that wheat, among all C3 crops, is known to be positively affected by increased CO₂ concentration. In the near-term (2021–2040), the projected average grain yield is increased from 4 to 6%, with increased CO₂ concentration from 429 to 456 ppm in the baseline period. The average grain yield is increased from 4 to 14% with the rise of CO₂ concentration from 436 to 569 ppm in mid-term scenarios compared with the historical baseline period. For long-term scenarios, with increasing CO₂ from 405 to 999 ppm, there is a 2 to 34% increase in future winter wheat grain yield compared with the baseline yield. The higher CO₂ concentration in the long-term under SSPs scenarios show more increase in grain yield than the near-term and mid-term. Amthor [92] noticed the 31% increase in wheat grain yield with increasing

CO₂ from 350 to 700 ppm. These outcomes are also in agreement with the findings of Helman and Bonfil [23], Ahmed et al. [93], and Ullah et al. [94] that increasing CO₂ level is beneficial for increasing the future grain yield. The increased CO₂ generally maximizes the crop yield by rising CO₂ concentration in the intercellular space (resulting in greater net photosynthesis) and reducing stomatal conductance (reducing transpiration) and increasing light-use and water-use efficiencies [95,96]. Climate change studies indicate that increased CO₂ levels could help crops maintain or possibly improve grain yields amid future climate change [97,98].

An optimal adaptation strategy would be required in the future to deal with the severe impacts of the warming climate. In the projected warming climate scenario, changing management methods, including planting dates, fertilizer rates, and irrigation applications, could help increase grain yield [52]. In this study, the CSM-CERES-Wheat model predicted the increase in grain yield under management scenarios of irrigation water, N fertilizer, and sowing dates in warming climatic conditions. The 260 mm irrigation water and farming practice 275 kg ha⁻¹ N fertilizer (W260N275) management scenario under the sowing of winter wheat on the recommended date of early October (this used the October 3 sowing date) showed a significant increase in grain yield compared to the average grain yield predicted by EC-Earth3 GCM in a warming climate. Similarly, Zheng et al. [99] suggested October 7 to 17 as the optimal sowing dates for winter wheat in Guanzhong in the Southern China Plain to increase grain yield. The rise in temperature and reduction in precipitation increases the evapotranspiration (ET) of the crop and lowers the moisture in the soil, which requires more irrigation water for the crop to maintain the soil moisture at an optimal level [100,101]. In this study, the increase in irrigation water and N fertilizer above 260 mm and 275 kg ha⁻¹ did not increase the grain yield in warm climatic conditions. When excessive irrigation water is used, nutrients are highly susceptible to leaching from the root zone and can negatively impact the grain yield [102]. Similar findings were observed by Rahman et al. [9] that a higher dose of N fertilizer and irrigation water did not significantly increase the crop yield in a warming climate. Choosing the optimal sowing date, irrigation water, and nitrogen fertilizer application can reduce the adverse effects of a warming climate [52,103]. Winter wheat yield can improve significantly in a warming climate in the near-term with the sowing of wheat on 3 October (which is earlier than the traditional planting) and by applying 30% more irrigation water than farming practice and farming practice with N fertilizer application.

Further, this study analyzed the performance of GCMs compared with observed using the Taylor diagram. Salehnia et al. [72], Ullah et al. [104], and Hamed et al. [73] also used a similar approach for examining the performance of the GCMs with observed climate data. Among all the GCMs in the near-term, ACCESS-CM2 can be the best GCM for maximum temperature and minimum temperature simulation in the study area climate compared to other GCMs under the SSP4.5 scenario. For the precipitation simulation, CanESM5 and ACCESS-CM2 can be the optimal GCMs under the SSP4.5 scenario in the near-term.

The current study successfully calibrated and evaluated the DSSAT CERES-Wheat model using two-year field experimental data and effectively examined the impact of climate change on future grain yield in the near-term, mid-term, and long-term under SSPs scenarios of CMIP6. Even though this study demonstrated success, its limitations include the uncertainty in GCMs climate projection [105]. Although there is a consensus among improved climatic models about changes in a projected rising temperature, the extent of these changes differs substantially. However, projections of precipitation changes are usually uncertain [88]. The GCM predicted climate change is uncertain due to various factors, including emission scenarios, model structure, downscaling techniques, bias correction methods, and impact models [106,107]. Therefore, further study is required to address the uncertainty in the GCM climate change projections by using more than five GCMs under various shared socioeconomic pathways scenarios. Other limitations include the current study using two growing season crop data from one experimental station for single crop model calibration and evaluation. Future work will use a multi-model ensemble and

multi-year experimental data from the different experimental stations for calibrating the crop model to reduce uncertainty.

5. Conclusions

The CSM DSSAT-CERES-Wheat model performed well in simulating the winter wheat phenology, grain yield, total dry matter, and harvest index. The findings indicate that temperature, precipitation, and the CO₂ increase positively impact the future winter wheat grain yield in the near-term, mid-term, and long-term. The interplay among these climatic factors suggests that the increase in precipitation and CO₂ offset the decrease in winter wheat grain yields because of the increased temperature in the future.

Several management scenarios were investigated to determine the best crop management practices to mitigate future climate change impacts on wheat grain yields. The mitigation of the negative effect of the warming climate on existing and future production systems requires better adaptation practices, including changing the sowing date, fertilizer rate, and irrigation amount for winter wheat. Our findings revealed that the sowing of winter wheat on 3 October and applying farmer's fertilizer application rate of nitrogen and 30% more irrigation water than farmer practice can be the optimal adaptive strategy in the near-term to mitigate the adverse impact of the warming climate on winter wheat grain yield in the North China Plain.

The limited observed data, uncertainties in GCMs, selecting only one agroclimatic zone, and the use of a single crop model are the apparent limitations of the study. Meanwhile, our investigations served their intended purpose. The future work will be conducted in different agroclimatic zones, and multi-year observed data will be collected to parametrize the crop models. Additionally, multi-model ensembles will be used to improve the accuracy and reduce the uncertainty of climate change effects in future research work.

Supplementary Materials: The following supporting information can be downloaded at: <https://www.mdpi.com/article/10.3390/atmos13081275/s1>, Figure S1: Taylor diagram for maximum temperature, minimum temperature, and precipitation for five GCMs under the SSP4.5 scenario in the near-term. s; Table S1: Projected CO₂ concentration increment under various SSPs scenarios as compared to historical baseline climate data in near-term, mid-term, and long-term; Table S2: Simulated and observed values of phenology, grain yield, total dry matter, and harvest index using the DSSAT-CERES-Wheat model for calibrated and evaluated treatments.

Author Contributions: Conceptualization, H.Y., M.R.S. and D.C.; methodology, M.R.S., M.H.-u.-R. and M.S.; software, M.R.S., D.C. and M.H.-u.-R.; validation, H.Y., M.H.-u.-R. and M.S.; formal analysis, M.R.S., D.C. and M.S.; investigation, H.Y., M.H.-u.-R. and M.S.; resources, H.Y., D.C. and M.H.-u.-R.; writing—original draft preparation, M.R.S., D.C. and H.Y.; writing—review and editing, H.Y., M.H.-u.-R. and M.S. All authors have read and agreed to the published version of the manuscript.

Funding: The authors are thankful to the Key Research and Development Program of Hebei Province (Grant No. 21327002D, 20327003D) and the National Key Research and Development Program of China (Grant No. 2017YFD0201502).

Institutional Review Board Statement: Not applicable.

Informed Consent Statement: Not applicable.

Data Availability Statement: The historical meteorological data for 20 years, including daily precipitation, solar radiation, and maximum–minimum air temperature from 1995 to 2014, can be collected from China Meteorological Data Sharing Service System: <http://cdc.cma.gov.cn> (accessed on 10 October 2021). The global climate model data under SSP4.5 and SSP8.5 scenarios of CMIP6 can be obtained from the Earth System Grid Federation (ESGF) website: <https://esgf-node.llnl.gov/search/cmip6/> (accessed on 25 October 2021).

Conflicts of Interest: The authors declare no conflict of interest.

References

- Dubey, M.; Mishra, A.; Singh, R. Climate change impact analysis using bias-corrected multiple global climate models on rice and wheat yield. *J. Water Clim. Chang.* **2021**, *12*, 1282–1296. [\[CrossRef\]](#)
- Cui, J.; Glatzel, S.; Bruckman, V.J.; Wang, B.; Lai, D.Y.F. Long-term effects of biochar application on greenhouse gas production and microbial community in temperate forest soils under increasing temperature. *Sci. Total Environ.* **2021**, *767*, 145021. [\[CrossRef\]](#) [\[PubMed\]](#)
- IPCC. *IPCC Special Report on the Ocean and Cryosphere in a Changing Climate*; Pörtner, H.-O., Roberts, D.C., Masson-Delmotte, V., Zhai, P., Tignor, M., Poloczanska, E., Mintenbeck, K., Alegria, A., Nicolai, M., Okem, A., et al., Eds.; 2019; *in press*.
- Ahmad, I.; Ahmad, B.; Boote, K.; Hoogenboom, G. Adaptation strategies for maize production under climate change for semi-arid environments. *Eur. J. Agron.* **2020**, *115*, 126040. [\[CrossRef\]](#)
- Xu, C.; Lu, C.; Sun, Q. Impact of climate change on irrigation water requirement of wheat growth—A case study of the Beijing-Tianjin-Hebei region in China. *Urban Clim.* **2021**, *39*, 100971. [\[CrossRef\]](#)
- IPCC. *Climate Change 2014: Mitigation of Climate Change: Working Group III Contribution to the IPCC Fifth Assessment Report*; 9781107058217; Cambridge University Press: Cambridge, UK, 2015.
- Gul, F.; Ahmed, I.; Ashfaq, M.; Jan, D.; Fahad, S.; Li, X.; Wang, D.; Fahad, M.; Fayyaz, M.; Shah, S.A. Use of crop growth model to simulate the impact of climate change on yield of various wheat cultivars under different agro-environmental conditions in Khyber Pakhtunkhwa, Pakistan. *Arab. J. Geosci.* **2020**, *13*, 1–14. [\[CrossRef\]](#)
- Lal, R. *Climate Change and Agriculture*; Elsevier: Amsterdam, The Netherlands, 2021; pp. 661–686.
- Rahman, M.H.u.; Ahmad, A.; Wang, X.; Wajid, A.; Nasim, W.; Hussain, M.; Ahmad, B.; Ahmad, I.; Ali, Z.; Ishaque, W. Multi-model projections of future climate and climate change impacts uncertainty assessment for cotton production in Pakistan. *Agric. For. Meteorol.* **2018**, *253*, 94–113. [\[CrossRef\]](#)
- Ma, L.; Fang, Q.X.; Sima, M.W.; Burkey, K.O.; Harmel, R.D. Simulated climate change effects on soybean production using two crop modules in RZWQM2. *Agron. J.* **2021**, *113*, 1349–1365. [\[CrossRef\]](#)
- Ahmed, I.; ur Rahman, M.H.; Ahmed, S.; Hussain, J.; Ullah, A.; Judge, J. Assessing the impact of climate variability on maize using simulation modeling under semi-arid environment of Punjab, Pakistan. *Environ. Sci. Pollut. Res.* **2018**, *25*, 28413–28430. [\[CrossRef\]](#)
- Shoukat, M.R.; Shafeeqe, M.; Sarwar, A. Investigating effects of deficit irrigation levels and fertilizer rates on water use efficiency and productivity based on field observations and modeling approaches. *Int. J. Hydrogen* **2021**, *5*, 252–263. [\[CrossRef\]](#)
- IPCC. *Climate Change 2013: The Physical Science Basis: Working Group I Contribution to the Fifth Assessment Report of the Intergovernmental Panel on Climate Change*; Cambridge University Press: Cambridge, UK, 2014.
- Liu, Q.; Niu, J.; Sivakumar, B.; Ding, R.; Li, S. Accessing future crop yield and crop water productivity over the Heihe River basin in northwest China under a changing climate. *Geosci. Lett.* **2021**, *8*, 1–16. [\[CrossRef\]](#)
- Bhattacharyya, P.; Pathak, H.; Pal, S. *Impact of Climate Change on Agriculture: Evidence and Predictions*; Springer: Berlin/Heidelberg, Germany, 2020; pp. 17–32.
- Olesen, J.E.; Trnka, M.; Kersebaum, K.C.; Skjelvåg, A.O.; Seguin, B.; Peltonen-Sainio, P.; Rossi, F.; Kozyra, J.; Micale, F. Impacts and adaptation of European crop production systems to climate change. *Eur. J. Agron.* **2011**, *34*, 96–112. [\[CrossRef\]](#)
- Zhang, Y.; Niu, H.; Yu, Q. Impacts of climate change and increasing carbon dioxide levels on yield changes of major crops in suitable planting areas in China by the 2050s. *Ecol. Indic.* **2021**, *125*, 107588. [\[CrossRef\]](#)
- Li, J.-p.; Zhang, Z.; Yao, C.-S.; Yang, L.I.U.; Wang, Z.-M.; Fang, B.-T.; Zhang, Y.-H. Improving winter wheat grain yield and water-/nitrogen-use efficiency by optimizing the micro-sprinkling irrigation amount and nitrogen application rate. *J. Integr. Agric.* **2021**, *20*, 606–621. [\[CrossRef\]](#)
- Zhang, T.; Huang, Y. Impacts of climate change and inter-annual variability on cereal crops in China from 1980 to 2008. *J. Sci. Food Agric.* **2012**, *92*, 1643–1652. [\[CrossRef\]](#) [\[PubMed\]](#)
- You, L.; Rosegrant, M.W.; Wood, S.; Sun, D. Impact of growing season temperature on wheat productivity in China. *Agric. For. Meteorol.* **2009**, *149*, 1009–1014. [\[CrossRef\]](#)
- Lopes, M.S. Will temperature and rainfall changes prevent yield progress in Europe? *Food Energy Secur.* **2022**, *31*, e372. [\[CrossRef\]](#)
- Rashid, M.A.; Jabloun, M.; Andersen, M.N.; Zhang, X.; Olesen, J.E. Climate change is expected to increase yield and water use efficiency of wheat in the North China Plain. *Agric. Water Manag.* **2019**, *222*, 193–203. [\[CrossRef\]](#)
- Helman, D.; Bonfil, D.J. Six decades of warming and drought in the world's top wheat-producing countries offset the benefits of rising CO₂ to yield. *Sci. Rep.* **2022**, *12*, 7921. [\[CrossRef\]](#)
- Liu, Y.; Li, N.; Zhang, Z.; Huang, C.; Chen, X.; Wang, F. The central trend in crop yields under climate change in China: A systematic review. *Sci. Total Environ.* **2020**, *704*, 135355. [\[CrossRef\]](#)
- Zhai, R.; Tao, F.; Lall, U.; Elliott, J. Africa would need to import more maize in the future even under 1.5 °C warming scenario. *Earth's Future* **2021**, *9*, e2020EF001574. [\[CrossRef\]](#)
- Wang, Z.-B.; Meng, C.-S.; Chen, J.; Chen, F. Risk Assessment of Crop Production Amid Climate Change Based on the Principle of Maximum Entropy: A Case Study of Winter Wheat Production on the North China Plain. *Int. J. Plant Prod.* **2019**, *13*, 275–284. [\[CrossRef\]](#)
- Lal, R.; Delgado, J.A.; Groffman, P.M.; Millar, N.; Dell, C.; Rotz, A. Management to mitigate and adapt to climate change. *J. Soil Water Conserv.* **2011**, *66*, 276–285. [\[CrossRef\]](#)

28. Tui, S.H.-K.; Descheemaeker, K.; Valdivia, R.O.; Masikati, P.; Sisito, G.; Moyo, E.N.; Crespo, O.; Ruane, A.C.; Rosenzweig, C. Climate change impacts and adaptation for dryland farming systems in Zimbabwe: A stakeholder-driven integrated multi-model assessment. *Clim. Chang.* **2021**, *168*, 1–21. [\[CrossRef\]](#)
29. Ding, Z.; Ali, E.F.; Elmahdy, A.M.; Ragab, K.E.; Seleiman, M.F.; Kheir, A.M.S. Modeling the combined impacts of deficit irrigation, rising temperature and compost application on wheat yield and water productivity. *Agric. Water Manag.* **2021**, *244*, 106626. [\[CrossRef\]](#)
30. Singh, A.P.; Dhadse, K. Economic evaluation of crop production in the Ganges region under climate change: A sustainable policy framework. *J. Clean. Prod.* **2021**, *278*, 123413. [\[CrossRef\]](#)
31. Srivastava, R.K.; Panda, R.K.; Chakraborty, A. Assessment of climate change impact on maize yield and yield attributes under different climate change scenarios in eastern India. *Ecol. Indic.* **2021**, *120*, 106881. [\[CrossRef\]](#)
32. Liu, W.; Ye, T.; Shi, P. Decreasing wheat yield stability on the North China Plain: Relative contributions from climate change in mean and variability. *Int. J. Climatol.* **2021**, *41*, E2820–E2833. [\[CrossRef\]](#)
33. Zheng, Z.; Cai, H.; Wang, Z.; Wang, X. Simulation of climate change impacts on phenology and production of winter wheat in Northwestern China using CERES-wheat model. *Atmosphere* **2020**, *11*, 681. [\[CrossRef\]](#)
34. Hoogenboom, G.; Porter, C.H.; Boote, K.J.; Shelia, V.; Wilkens, P.W.; Singh, U.; White, J.W.; Asseng, S.; Lizaso, J.I.; Moreno, L.P.; et al. The DSSAT crop modeling ecosystem. In *Advances in Crop Modelling for a Sustainable Agriculture*; Burleigh Dodds Science Publishing: Cambridge, UK, 2019; pp. 173–216. [\[CrossRef\]](#)
35. Jones, J.W.; Hoogenboom, G.; Porter, C.H.; Boote, K.J.; Batchelor, W.D.; Hunt, L.A.; Wilkens, P.W.; Singh, U.; Gijsman, A.J.; Ritchie, J.T. The DSSAT cropping system model. *Eur. J. Agron.* **2003**, *18*, 235–265. [\[CrossRef\]](#)
36. Saddique, Q.; Cai, H.; Ishaque, W.; Chen, H.; Chau, H.W.; Chattha, M.U.; Hassan, M.U.; Khan, M.I.; He, J. Optimizing the sowing date and irrigation strategy to improve maize yield by using CERES (Crop Estimation through Resource and Environment Synthesis)-maize model. *Agronomy* **2019**, *9*, 109. [\[CrossRef\]](#)
37. Asseng, S.; Martre, P.; Maiorano, A.; Rötter, R.P.; O’Leary, G.J.; Fitzgerald, G.J.; Girousse, C.; Motzo, R.; Giunta, F.; Babar, M.A. Climate change impact and adaptation for wheat protein. *Glob. Chang. Biol.* **2019**, *25*, 155–173. [\[CrossRef\]](#) [\[PubMed\]](#)
38. Asseng, S.; Kheir, A.M.; Kassie, B.T.; Hoogenboom, G.; Abdelaal, A.I.; Haman, D.Z.; Ruane, A.C. Can Egypt become self-sufficient in wheat? *Environ. Res. Lett.* **2018**, *13*, 094012. [\[CrossRef\]](#)
39. Saddique, Q.; Khan, M.I.; Habib ur Rahman, M.; Jiataun, X.; Waseem, M.; Gaiser, T.; Mohsin Waqas, M.; Ahmad, I.; Chong, L.; Cai, H. Effects of Elevated Air Temperature and CO₂ on Maize Production and Water Use Efficiency under Future Climate Change Scenarios in Shaanxi Province, China. *Atmosphere* **2020**, *11*, 843. [\[CrossRef\]](#)
40. Guo, Y.; Yu, X.; Xu, Y.-P.; Wang, G.; Xie, J.; Gu, H. A comparative assessment of CMIP5 and CMIP6 in hydrological responses of the Yellow River Basin, China. *Hydrol. Res.* **2022**, *53*, 867–891. [\[CrossRef\]](#)
41. Gusain, A.; Ghosh, S.; Karmakar, S. Added value of CMIP6 over CMIP5 models in simulating Indian summer monsoon rainfall. *Atmos. Res.* **2020**, *232*, 104680. [\[CrossRef\]](#)
42. Eyring, V.; Bony, S.; Meehl, G.A.; Senior, C.A.; Stevens, B.; Stouffer, R.J.; Taylor, K.E. Overview of the Coupled Model Intercomparison Project Phase 6 (CMIP6) experimental design and organization. *Geosci. Model Dev.* **2016**, *9*, 1937–1958. [\[CrossRef\]](#)
43. Zhu, H.; Jiang, Z.; Li, J.; Li, W.; Sun, C.; Li, L. Does CMIP6 inspire more confidence in simulating climate extremes over China? *Adv. Atmos. Sci.* **2020**, *37*, 1119–1132. [\[CrossRef\]](#)
44. O’Neill, B.C.; Tebaldi, C.; Vuuren, D.P.v.; Eyring, V.; Friedlingstein, P.; Hurtt, G.; Knutti, R.; Kriegler, E.; Lamarque, J.-F.; Lowe, J. The scenario model intercomparison project (ScenarioMIP) for CMIP6. *Geosci. Model Dev.* **2016**, *9*, 3461–3482. [\[CrossRef\]](#)
45. Rosenzweig, C.; Jones, J.W.; Hatfield, J.L.; Ruane, A.C.; Boote, K.J.; Thorburn, P.; Antle, J.M.; Nelson, G.C.; Porter, C.; Janssen, S. The agricultural model intercomparison and improvement project (AgMIP): Protocols and pilot studies. *Agric. For. Meteorol.* **2013**, *170*, 166–182. [\[CrossRef\]](#)
46. Zhai, J.; Mondal, S.K.; Fischer, T.; Wang, Y.; Su, B.; Huang, J.; Tao, H.; Wang, G.; Ullah, W.; Uddin, M.J. Future drought characteristics through a multi-model ensemble from CMIP6 over South Asia. *Atmos. Res.* **2020**, *246*, 105111. [\[CrossRef\]](#)
47. Zadoks, J.C.; Chang, T.T.; Konzak, C.F. A decimal code for the growth stages of cereals. *Weed Res.* **1974**, *14*, 415–421. [\[CrossRef\]](#)
48. Malik, W.; Isla, R.; Dechmi, F. DSSAT-CERES-maize modelling to improve irrigation and nitrogen management practices under Mediterranean conditions. *Agric. Water Manag.* **2019**, *213*, 298–308. [\[CrossRef\]](#)
49. Rahman, M.H.-u.; Ahmad, A.; Wajid, A.; Hussain, M.; Rasul, F.; Ishaque, W.; Islam, M.A.; Shelia, V.; Awais, M.; Ullah, A. Application of CSM-CROPGRO-Cotton model for cultivars and optimum planting dates: Evaluation in changing semi-arid climate. *Field Crops Res.* **2019**, *238*, 139–152. [\[CrossRef\]](#)
50. Rahman, M.H.-u.; Raza, A.; Ahrends, H.E.; Hüging, H.; Gaiser, T. Impact of in-field soil heterogeneity on biomass and yield of winter triticale in an intensively cropped hummocky landscape under temperate climate conditions. *Precis. Agric.* **2022**, *23*, 912–938. [\[CrossRef\]](#)
51. Jones, J.W.; He, J.; Boote, K.J.; Wilkens, P.; Porter, C.H.; Hu, Z. Estimating DSSAT cropping system cultivar-specific parameters using Bayesian techniques. *Methods Introd. Syst. Models Agric. Res.* **2011**, *2*, 365–393.
52. Yasin, M.; Ahmad, A.; Khaliq, T.; Habib-ur-Rahman, M.; Niaz, S.; Gaiser, T.; Ghafoor, I.; Qasim, M.; Hoogenboom, G. Climate change impact uncertainty assessment and adaptations for sustainable maize production using multi-crop and climate models. *Environ. Sci. Pollut. Res.* **2022**, *29*, 18967–18988. [\[CrossRef\]](#) [\[PubMed\]](#)

53. Si, Z.; Zain, M.; Li, S.; Liu, J.; Liang, Y.; Gao, Y.; Duan, A. Optimizing nitrogen application for drip-irrigated winter wheat using the DSSAT-CERES-Wheat model. *Agric. Water Manag.* **2021**, *244*, 106592. [\[CrossRef\]](#)
54. Hussain, J.; Khaliq, T.; Rahman, M.H.U.; Ullah, A.; Ahmed, I.; Srivastava, A.K.; Gaiser, T.; Ahmad, A. Effect of temperature on sowing dates of wheat under arid and semi-arid climatic regions and impact quantification of climate change through mechanistic modeling with evidence from field. *Atmosphere* **2021**, *12*, 927. [\[CrossRef\]](#)
55. He, W.; Yang, J.Y.; Drury, C.F.; Smith, W.N.; Grant, B.B.; He, P.; Qian, B.; Zhou, W.; Hoogenboom, G. Estimating the impacts of climate change on crop yields and N₂O emissions for conventional and no-tillage in Southwestern Ontario, Canada. *Agric. Syst.* **2018**, *159*, 187–198. [\[CrossRef\]](#)
56. Leghari, S.J.; Hu, K.; Wei, Y.; Wang, T.; Bhutto, T.A.; Buriro, M. Modelling water consumption, N fates and maize yield under different water-saving management practices in China and Pakistan. *Agric. Water Manag.* **2021**, *255*, 107033. [\[CrossRef\]](#)
57. Moriasi, D.N.; Arnold, J.G.; Van Liew, M.W.; Bingner, R.L.; Harmel, R.D.; Veith, T.L. Model evaluation guidelines for systematic quantification of accuracy in watershed simulations. *Trans. ASABE* **2007**, *50*, 885–900. [\[CrossRef\]](#)
58. Yao, F.-M.; Li, Q.-Y.; Zeng, R.-Y.; Shi, S.-Q. Effects of different agricultural treatments on narrowing winter wheat yield gap and nitrogen use efficiency in China. *J. Integr. Agric.* **2021**, *20*, 383–394. [\[CrossRef\]](#)
59. Mukaka, M.M. Statistics corner: A guide to appropriate use of correlation coefficient in medical research. *Malawi Med. J.* **2012**, *24*, 69–71.
60. Ullah, A.; Ahmad, I.; Habib ur, R.; Saeed, U.; Ahmad, A.; Mahmood, A.; Hoogenboom, G. *Climate Smart Interventions of Small-Holder Farming Systems*; IntechOpen: London, UK, 2019; pp. 1–14.
61. IPCC. *Climate Change 2021: The Physical Science Basis. Contribution of Working Group I to the Sixth Assessment Report of the Intergovernmental Panel on Climate Change*; 9789291691586; Cambridge University Press: Cambridge, UK, 2021; p. 3949, *in press*.
62. Tebaldi, C.; Debeire, K.; Eyring, V.; Fischer, E.; Fyfe, J.; Friedlingstein, P.; Knutti, R.; Lowe, J.; O'Neill, B.; Sanderson, B. Climate model projections from the scenario model intercomparison project (ScenarioMIP) of CMIP6. *Earth Syst. Dyn.* **2021**, *12*, 253–293. [\[CrossRef\]](#)
63. Iqbal, Z.; Shahid, S.; Ahmed, K.; Ismail, T.; Ziarh, G.F.; Chung, E.-S.; Wang, X. Evaluation of CMIP6 GCM rainfall in mainland Southeast Asia. *Atmos. Res.* **2021**, *254*, 105525. [\[CrossRef\]](#)
64. Grose, M.R.; Narsey, S.; Delage, F.P.; Dowdy, A.J.; Bador, M.; Boschat, G.; Chung, C.; Kajtar, J.B.; Rauniyar, S.; Freund, M.B. Insights from CMIP6 for Australia's future climate. *Earth's Future* **2020**, *8*, e2019EF001469. [\[CrossRef\]](#)
65. Riahi, K.; Van Vuuren, D.P.; Kriegler, E.; Edmonds, J.; O'Neill, B.C.; Fujimori, S.; Bauer, N.; Calvin, K.; Dellink, R.; Fricko, O. The shared socioeconomic pathways and their energy, land use, and greenhouse gas emissions implications: An overview. *Glob. Environ. Chang.* **2017**, *42*, 153–168. [\[CrossRef\]](#)
66. Wetterhall, F.; Pappenberger, F.; He, Y.; Freer, J.; Cloke, H.L. Conditioning model output statistics of regional climate model precipitation on circulation patterns. *Nonlinear Processes Geophys.* **2012**, *19*, 623–633. [\[CrossRef\]](#)
67. Salehnia, N.; Hosseini, F.; Farid, A.; Kolsoumi, S.; Zarrin, A.; Hasheminia, M. Comparing the performance of dynamical and statistical downscaling on historical run precipitation data over a semi-arid region. *Asia-Pac. J. Atmos. Sci.* **2019**, *55*, 737–749. [\[CrossRef\]](#)
68. Fan, X.; Jiang, L.; Gou, J. Statistical downscaling and projection of future temperatures across the Loess Plateau, China. *Weather Clim. Extrem.* **2021**, *32*, 100328. [\[CrossRef\]](#)
69. Liang, Z.; Zhang, L.; Li, W.; Zhang, J.; Frewer, L.J. Adoption of combinations of adaptive and mitigatory climate-smart agricultural practices and its impacts on rice yield and income: Empirical evidence from Hubei, China. *Clim. Risk Manag.* **2021**, *32*, 100314. [\[CrossRef\]](#)
70. Onyutha, C.; Asiimwe, A.; Ayugi, B.; Ngoma, H.; Ongoma, V.; Tabari, H. Observed and future precipitation and evapotranspiration in water management zones of Uganda: CMIP6 projections. *Atmosphere* **2021**, *12*, 887. [\[CrossRef\]](#)
71. Taylor, K.E. Summarizing multiple aspects of model performance in a single diagram. *J. Geophys. Res. Atmos.* **2001**, *106*, 7183–7192. [\[CrossRef\]](#)
72. Salehnia, N.; Salehnia, N.; Saradari Torshizi, A.; Kolsoumi, S. Rainfed wheat (*Triticum aestivum* L.) yield prediction using economical, meteorological, and drought indicators through pooled panel data and statistical downscaling. *Ecol. Indic.* **2020**, *111*, 105991. [\[CrossRef\]](#)
73. Hamed, M.M.; Nashwan, M.S.; Shahid, S.; bin Ismail, T.; Wang, X.-j.; Dewan, A.; Asaduzzaman, M. Inconsistency in historical simulations and future projections of temperature and rainfall: A comparison of CMIP5 and CMIP6 models over Southeast Asia. *Atmos. Res.* **2022**, *265*, 105927. [\[CrossRef\]](#)
74. Wootten, A.M.; Dixon, K.W.; Adams-Smith, D.J.; McPherson, R.A. Statistically downscaled precipitation sensitivity to gridded observation data and downscaling technique. *Int. J. Climatol.* **2021**, *41*, 980–1001. [\[CrossRef\]](#)
75. Jiang, R.; He, W.; Zhou, W.; Hou, Y.; Yang, J.Y.; He, P. Exploring management strategies to improve maize yield and nitrogen use efficiency in northeast China using the DNDC and DSSAT models. *Comput. Electron. Agric.* **2019**, *166*, 104988. [\[CrossRef\]](#)
76. Zhang, D.; Li, R.; Batchelor, W.D.; Ju, H.; Li, Y. Evaluation of limited irrigation strategies to improve water use efficiency and wheat yield in the North China Plain. *PLoS ONE* **2018**, *13*, e0189989. [\[CrossRef\]](#)
77. Zhang, X.; Xiao, G.; Li, H.; Wang, L.; Wu, S.; Wu, W.; Meng, F. Mitigation of greenhouse gas emissions through optimized irrigation and nitrogen fertilization in intensively managed wheat–maize production. *Sci. Rep.* **2020**, *10*, 1–10. [\[CrossRef\]](#)

78. Fang, S.; Su, H.; Liu, W.; Tan, K.; Ren, S. Infrared warming reduced winter wheat yields and some physiological parameters, which were mitigated by irrigation and worsened by delayed sowing. *PLoS ONE* **2013**, *8*, e67518. [\[CrossRef\]](#)
79. Jia, D.; Wang, C.; Han, Y.; Huang, H.; Xiao, H. Impact of Climate Change on the Yield and Water Footprint of Winter Wheat in the Haihe River Basin, China. *Atmosphere* **2022**, *13*, 630. [\[CrossRef\]](#)
80. Li, Y.; Hou, R.; Liu, X.; Chen, Y.; Tao, F. Changes in wheat traits under future climate change and their contributions to yield changes in conventional vs. conservation tillage systems. *Sci. Total Environ.* **2022**, *815*, 152947. [\[CrossRef\]](#) [\[PubMed\]](#)
81. Timsina, J.; Humphreys, E. Performance of CERES-Rice and CERES-Wheat models in rice–wheat systems: A review. *Agric. Syst.* **2006**, *90*, 5–31. [\[CrossRef\]](#)
82. Feng, H.; Li, Z.; He, P.; Jin, X.; Yang, G.; Yu, H.; Yang, F. Simulation of Winter Wheat Phenology in Beijing Area with DSSAT-CERES Model. In Proceedings of the International Conference on Computer and Computing Technologies in Agriculture, Beijing, China, 27–30 September 2015; pp. 259–268.
83. Malik, W.; Dechmi, F. DSSAT modelling for best irrigation management practices assessment under Mediterranean conditions. *Agric. Water Manag.* **2019**, *216*, 27–43. [\[CrossRef\]](#)
84. IPCC. *Climate Change 2007: Impacts, Adaptation and Vulnerability. Contribution of Working Group II to the Fourth Assessment Report of the Intergovernmental Panel on Climate Change*; Parry, M.L., Canziani, O.F., Palutikof, J.P., van der Linden, P.J., Hanson, C.E., Eds.; 9780080449104; Cambridge University Press: Cambridge, UK, 2007.
85. Asseng, S.; Ewert, F.; Rosenzweig, C.; Jones, J.W.; Hatfield, J.L.; Ruane, A.C.; Boote, K.J.; Thorburn, P.J.; Rötter, R.P.; Cammarano, D. Uncertainty in simulating wheat yields under climate change. *Nat. Clim. Chang.* **2013**, *3*, 827–832. [\[CrossRef\]](#)
86. Kukal, M.S.; Irmak, S. Climate-driven crop yield and yield variability and climate change impacts on the US Great Plains agricultural production. *Sci. Rep.* **2018**, *8*, 1–18. [\[CrossRef\]](#) [\[PubMed\]](#)
87. Zhang, Y.; Shou, W.; Maucieri, C.; Lin, F. Rainfall increasing offsets the negative effects of nighttime warming on GHGs and wheat yield in North China Plain. *Sci. Rep.* **2021**, *11*, 6505. [\[CrossRef\]](#)
88. Zhao, C.; Liu, B.; Piao, S.; Wang, X.; Lobell, D.B.; Huang, Y.; Huang, M.; Yao, Y.; Bassu, S.; Ciais, P. Temperature increase reduces global yields of major crops in four independent estimates. *Proc. Natl. Acad. Sci. USA* **2017**, *114*, 9326–9331. [\[CrossRef\]](#)
89. Tao, F.; Zhang, Z.; Zhang, S.; Rötter, R.P.; Shi, W.; Xiao, D.; Liu, Y.; Wang, M.; Liu, F.; Zhang, H. Historical data provide new insights into response and adaptation of maize production systems to climate change/variability in China. *Field Crops Res.* **2016**, *185*, 1–11. [\[CrossRef\]](#)
90. Wang, Z.; Zhang, T.Q.; Tan, C.S.; Xue, L.; Bukovsky, M.; Qi, Z.M. Modeling impacts of climate change on crop yield and phosphorus loss in a subsurface drained field of Lake Erie region, Canada. *Agric. Syst.* **2021**, *190*, 103110. [\[CrossRef\]](#)
91. Kimball, B.; Kobayashi, K.; Bindi, M. Responses of agricultural crops to free-air CO₂ enrichment. *Adv. Agron.* **2002**, *77*, 293–368.
92. Amthor, J.S. Effects of atmospheric CO₂ concentration on wheat yield: Review of results from experiments using various approaches to control CO₂ concentration. *Field Crops Res.* **2001**, *73*, 1–34. [\[CrossRef\]](#)
93. Ahmed, M.; Akram, M.N.; Asim, M.; Aslam, M.; Hassan, F.-U.; Higgins, S.; Stöckle, C.O.; Hoogenboom, G. Calibration and validation of APSIM-Wheat and CERES-Wheat for spring wheat under rainfed conditions: Models evaluation and application. *Comput. Electron. Agric.* **2016**, *123*, 384–401. [\[CrossRef\]](#)
94. Ullah, A.; Ahmad, I.; Ahmad, A.; Khaliq, T.; Saeed, U.; Habib-ur-Rahman, M.; Hussain, J.; Ullah, S.; Hoogenboom, G. Assessing climate change impacts on pearl millet under arid and semi-arid environments using CSM-CERES-Millet model. *Environ. Sci. Pollut. Res.* **2019**, *26*, 6745–6757. [\[CrossRef\]](#) [\[PubMed\]](#)
95. Asseng, S.; Jamieson, P.D.; Kimball, B.; Pinter, P.; Sayre, K.; Bowden, J.W.; Howden, S.M. Simulated wheat growth affected by rising temperature, increased water deficit and elevated atmospheric CO₂. *Field Crops Res.* **2004**, *85*, 85–102. [\[CrossRef\]](#)
96. Drake, B.G.; Gonzalez-Meler, M.A.; Long, S.P. MORE EFFICIENT PLANTS: A Consequence of Rising Atmospheric CO₂? *Annu. Rev. Plant Physiol. Plant Mol. Biol.* **1997**, *48*, 609–639. [\[CrossRef\]](#)
97. Sommer, R.; Glazirina, M.; Yuldashev, T.; Otarov, A.; Ibraeva, M.; Martynova, L.; Bekenov, M.; Kholov, B.; Ibragimov, N.; Kobilov, R. Impact of climate change on wheat productivity in Central Asia. *Agric. Ecosyst. Environ.* **2013**, *178*, 78–99. [\[CrossRef\]](#)
98. Singh, P.; Nedumaran, S.; Ntare, B.R.; Boote, K.J.; Singh, N.P.; Srinivas, K.; Bantilan, M.C.S. Potential benefits of drought and heat tolerance in groundnut for adaptation to climate change in India and West Africa. *Mitig. Adapt. Strateg. Glob. Chang.* **2014**, *19*, 509–529. [\[CrossRef\]](#)
99. Zheng, Z.; Hoogenboom, G.; Cai, H.; Wang, Z. Winter wheat production on the Guanzhong Plain of Northwest China under projected future climate with SimCLIM. *Agric. Water Manag.* **2020**, *239*, 106233. [\[CrossRef\]](#)
100. Warsame, A.A.; Sheik-Ali, I.A.; Ali, A.O.; Sarkodie, S.A. Climate change and crop production nexus in Somalia: An empirical evidence from ARDL technique. *Environ. Sci. Pollut. Res.* **2021**, *28*, 19838–19850. [\[CrossRef\]](#)
101. Svoboda, N.; Strer, M.; Hufnagel, J. Rainfed winter wheat cultivation in the North German Plain will be water limited under climate change until 2070. *Environ. Sci. Eur.* **2015**, *27*, 1–7. [\[CrossRef\]](#) [\[PubMed\]](#)
102. Abd-Elrahman, S.H.; Saady, H.S.; El-Fattah, D.A.A.; Hashem, F.A.E. Effect of irrigation water and organic fertilizer on reducing nitrate accumulation and boosting lettuce productivity. *J. Soil Sci. Plant Nutr.* **2022**, *22*, 2144–2155. [\[CrossRef\]](#)
103. Raza, A.; Razzaq, A.; Mehmood, S.S.; Zou, X.; Zhang, X.; Lv, Y.; Xu, J. Impact of climate change on crops adaptation and strategies to tackle its outcome: A review. *Plants* **2019**, *8*, 34. [\[CrossRef\]](#) [\[PubMed\]](#)

104. Ullah, A.; Salehnia, N.; Kolsoumi, S.; Ahmad, A.; Khaliq, T. Prediction of effective climate change indicators using statistical downscaling approach and impact assessment on pearl millet (*Pennisetum glaucum* L.) yield through Genetic Algorithm in Punjab, Pakistan. *Ecol. Indic.* **2018**, *90*, 569–576. [[CrossRef](#)]
105. Wang, W.; Yuan, S.; Wu, C.; Yang, S.; Zhang, W.; Xu, Y.; Gu, J.; Zhang, H.; Wang, Z.; Yang, J. Field experiments and model simulation based evaluation of rice yield response to projected climate change in Southeastern China. *Sci. Total Environ.* **2021**, *761*, 143206. [[CrossRef](#)]
106. Leng, G.; Tang, Q.; Rayburg, S. Climate change impacts on meteorological, agricultural and hydrological droughts in China. *Glob. Planet. Chang.* **2015**, *126*, 23–34. [[CrossRef](#)]
107. Whitfield, S. Uncertainty, ignorance and ambiguity in crop modelling for African agricultural adaptation. *Clim. Chang.* **2013**, *120*, 325–340. [[CrossRef](#)]